

FACULDADE DE ENGENHARIA DA UNIVERSIDADE DO PORTO

Vehicle Tracking in Warehouses via Bluetooth Beacon Angle-of-Arrival

Telmo Francisco da Costa Soares



Mestrado Integrado em Engenharia Eletrotécnica e de Computadores

Supervisor: Dr. Nuno Miguel Cardanha Paulino

Second Supervisor: Dr. Luís Manuel de Sousa Pessoa

April 1, 2021

Abstract

During the last decade, significant progress has been made in the accuracy of indoor location and tracking systems. These advances are a response to the increased demand for accurate positioning systems, for applications such as staff and inventory tracking and management. These kinds of applications require accurate and reliable real-time indoor positioning systems with low implementation costs.

Indoor environments have distinct characteristics from outdoor environments, where Global Position System (GPS) has been extensively used. The inability to penetrate buildings makes this technology unsuitable for indoor positioning. Thus, a large variety of radio-frequency (RF) based technologies have been proposed as viable solutions, such as RFID, WiFi, Bluetooth, and Ultra Wide Band (UWB). However, no widely adopted solution has emerged.

Bluetooth is one of the most thriving technologies due to its low cost and power efficiency. Most Bluetooth-based locating systems rely on the received signal strength indicator (RSSI) to estimate the distance between a transmitter and a receiver. However, due to fluctuations of the RSSI measurements, high accuracies are not yet achieved. In the recently released Bluetooth 5.1 specification, the Bluetooth Special Interest Group (SIG) introduced a direction-finding feature which enables new solutions for Bluetooth-based indoor positioning.

In this thesis, an extensive study for indoor positioning and indoor tracking using the Bluetooth Angle of Arrival (AoA) capabilities is presented. This is accomplished using a simulator based on empirical samples retrieved from a commercial Bluetooth Low Energy (BLE) 5.1 solution. The proposed solution is based on a network topology with fixed low-cost beacons with omnidirectional antennas, and mobile receivers with antenna arrays. The receivers read periodic transmissions from the beacons, and can autonomously compute their position using trivial geometry. The need for a centralized system, which is present in existing location solutions based on AoA, is bypassed. The grid of fixed beacons can scale easily and at low cost; and can be deployed in locations without wall-power infrastructure. Additionally, the location algorithms are tolerant to beacon failures.

Tracking is achievable using a Kalman Filter (KF) to smooth the measured positions along the trajectory. A Dead Reckoning technique is also used to predict the location of the mobile receiver while new position estimations from AoA data are not available, using inertial measurements.

Lastly, the results of the tracking performance are presented. Here multiple scenarios were explored, i.e. multiple room layouts in conjunction with multiple forklift trajectories and different packet management policies. The performance metric is the system's accuracy measured by the root mean squared error (RMSE) of the estimated position relative to the real position. We demonstrate that sub-meter positioning accuracy is possible using only 50 beacons for a receiver moving

at a velocity of 10 meters per second.

Keywords: Angle of Arrival, Bluetooth Low Energy, Direction Finding, Indoor Positioning Systems, Indoor tracking, Kalman Filter

Resumo

Durante a última década, foi realizado um progresso significativo na precisão de sistemas de localização e rastreamento *indoor*. Estes avanços são uma resposta ao aumento da demanda por sistemas de posicionamento precisos, em aplicações como rastreamento e gestão de inventário e pessoal. Estes tipos de aplicações requerem sistemas de posicionamento *indoor* em tempo real fiáveis e precisos com baixos custos de implementação.

Ambientes *indoor* têm características diferentes de ambientes *outdoor*, onde o sistema de posicionamento global (GPS) tem sido usado extensivamente. A incapacidade de penetrar edifícios faz com que esta tecnologia seja inadequada para posicionamento *indoor*. Assim, uma grande variedade de tecnologias baseadas em radio frequência têm sido propostas como soluções viáveis, tais como RFID, WiFi, Bluetooth, e Ultra Wide Band (UWB). Contudo, não surgiu nenhuma solução amplamente adotada.

Bluetooth é uma das tecnologias mais prósperas devido ao seu baixo custo e eficiência energética. A maioria dos sistemas de localização baseados em Bluetooth dependem do indicador da força do sinal recebido para estimar a distância entre o transmissor e o recetor. No entanto, devido a flutuações nas medições do RSSI, altas precisões ainda não foram alcançadas. Na especificação Bluetooth 5.1 lançada recentemente, o Bluetooth Special Interest Group (SIG) introduziu um recurso de radiogoniometria que permite novas soluções para posicionamento *indoor* baseado em Bluetooth.

Nesta tese, é apresentado um estudo extensivo para posicionamento e rastreamento *indoor* usando as capacidades do ângulo de chegada do Bluetooth. Isto é realizado usando um simulador baseado em amostras empíricas retiradas de uma solução Bluetooth Low Energy (BLE) 5.1 comercial. A solução proposta é baseada numa topologia de rede com *beacons* fixos de baixo custo com antenas omnidirecionais, e recetores móveis com *arrays* de antenas. Os recetores leem as transmissões periódicas dos *beacons*, e conseguem calcular autonomamente as suas posições usando geometria trivial. A necessidade de um sistema centralizado, que está presente nas soluções de localização existentes baseadas em ângulo de chegada, é contornada. A grelha de *beacons* fixos é facilmente escalável e a baixo custo, e pode ser implementada em locais com uma infraestrutura sem paredes com tomadas elétricas. Adicionalmente, os algoritmos de localização são toleráveis a falhas nos *beacons*.

Rastreamento é conseguido usando um filtro de Kalman (KF) para suavizar as posições estimadas ao longo da trajetória. Uma técnica de Dead Reckoning é também usada para prever a localização do recetor móvel enquanto novas estimativas de posição dos dados de ângulo de chegada não estão disponíveis, usando medições inerciais.

Por fim, os resultados do desempenho do rastreamento são apresentados. Aqui, múltiplos cenários são explorados, isto é, múltiplos esquemas de espaço em conjunto com múltiplas trajetórias de empilhadora e diferentes políticas de gestão de pacotes. A métrica de desempenho é a precisão do sistema medida pela raiz quadrada do erro médio da posição estimada relativa

à posição real. Demonstrámos que uma precisão abaixo de um metro é possível quando usados apenas 50 *beacons* para um recetor movendo-se a uma velocidade de 10 metros por segundo.

Palavras-Chave: Ângulo de chegada, Bluetooth Low Energy, Radiogoniometria, Sistemas de posicionamento *indoor*, Rastreamento *indoor*, Filtro de Kalman

Acknowledgements

As one important chapter of my life is coming to an end, I cannot express enough how grateful I am to everyone who helped me get here.

First of all, a special thank you to my Supervisor Dr. Nuno Paulino, and Second Supervisor Dr. Luís Pessoa for the guidance provided during this dissertation.

Secondly to my parents for making me the person I am today, and for all the support provided during the course, that made all of this possible.

Thank you also:

To my teachers since my elementary school teacher D. Irene, to my teachers at the FEUP.

To all my colleagues, who accompanied me on this journey, especially José, João, and André, that were a great company during classes, group works, and breaks.

To my old housemates Ricardo and Manuel, that made my university life much more amusing.

To my longtime friends Jacinta and Sónia, who made travels to university less boring.

Telmo Soares

*“If you can dream it,
you can do it.”*

Walt Disney

Contents

1	Introduction	1
1.1	Context	1
1.2	Objectives	2
1.3	Motivation	2
1.4	Document structure	2
2	Related Work	3
2.1	Background	3
2.1.1	Wireless indoor tracking	3
2.1.2	Performance Metrics	3
2.1.3	Indoor location techniques	4
2.1.4	Overview of the existing technologies	9
2.1.5	Summary	11
2.2	Literature Review	11
3	Simulator	13
3.1	Simulator Description	13
3.2	Simulator Architecture	14
3.2.1	Room	15
3.2.2	Beacon	16
3.2.3	Packet	16
3.2.4	Forklift	16
4	Results	25
4.1	Experimental Setup	25
4.2	Defining the Uncertainty value	25
4.2.1	Experiment A: Uncertainty vs. Beacon Period	25
4.3	Defining the Minimum Number of Packets	26
4.3.1	Experiment B: Minimum Number of Packets vs. Number of Beacons	27
4.3.2	Experiment C: Minimum Number of Packets vs. Beacon Period	28
4.4	Evaluation of tracking performance	29
4.4.1	Experiment D: Tracking Evaluation on a Sinusoidal Trajectory	30
4.4.2	Experiment E: Tracking Evaluation on a Parabolic Trajectory	31
4.4.3	Experiment F: Tracking Evaluation on a Linear Trajectory	31
5	Conclusions and Future Work	33
5.1	Conclusions	33
5.2	Future Work	34

A Trajectory	35
A.1 Trajectories	35
References	45

List of Figures

2.1	Example of trilateration with three beacons, adapted from [2].	5
2.2	Position estimation based on ToA measurements.	6
2.3	Position estimation based on TDoA measurements.	7
2.4	Position estimation based on AoA technique, adapted from [1]	8
2.5	AoA based localization.	8
3.1	Antenna array based on the TLSR8258 [17].	17
3.2	Results for a Telink kit in indoor environment [17].	18
3.3	Estimated position using least squares method in comparison with real position [17].	19
3.4	Flowchart of the system.	24
4.1	Sweep of the Kalman uncertainty.	27
4.2	Minimum packet size sweep for different number of beacons.	27
4.3	Minimum packet size sweep for different beacon periods.	28
4.4	Logarithmic regression of minimum packet dependency on beacon period	29
4.5	Tracking performance on Experiment D.	30
4.6	Tracking performance on Experiment E	31
4.7	Tracking performance on Experiment F	32
A.1	Label of the figures.	35
A.2	Sinusoidal trajectory with 16 beacons.	35
A.3	Sinusoidal trajectory with 20 beacons.	36
A.4	Sinusoidal trajectory with 24 beacons.	36
A.5	Sinusoidal trajectory with 28 beacons.	36
A.6	Sinusoidal trajectory with 32 beacons.	36
A.7	Sinusoidal trajectory with 36 beacons.	36
A.8	Sinusoidal trajectory with 40 beacons.	36
A.9	Sinusoidal trajectory with 44 beacons.	36
A.10	Sinusoidal trajectory with 48 beacons.	36
A.11	Sinusoidal trajectory with 52 beacons.	36
A.12	Sinusoidal trajectory with 56 beacons.	36
A.13	Sinusoidal trajectory with 60 beacons.	36
A.14	Sinusoidal trajectory with 64 beacons.	36
A.15	Parabolic trajectory with 16 beacons.	37
A.16	Parabolic trajectory with 20 beacons.	37
A.17	Parabolic trajectory with 24 beacons.	37
A.18	Parabolic trajectory with 28 beacons.	37
A.19	Parabolic trajectory with 32 beacons.	38
A.20	Parabolic trajectory with 36 beacons.	38

A.21 Parabolic trajectory with 40 beacons.	38
A.22 Parabolic trajectory with 44 beacons.	38
A.23 Parabolic trajectory with 48 beacons.	39
A.24 Parabolic trajectory with 52 beacons.	39
A.25 Parabolic trajectory with 56 beacons.	39
A.26 Parabolic trajectory with 60 beacons.	39
A.27 Parabolic trajectory with 64 beacons.	40
A.28 Linear trajectory with 16 beacons.	40
A.29 Linear trajectory with 20 beacons.	40
A.30 Linear trajectory with 24 beacons.	41
A.31 Linear trajectory with 28 beacons.	41
A.32 Linear trajectory with 32 beacons.	41
A.33 Linear trajectory with 36 beacons.	41
A.34 Linear trajectory with 40 beacons.	41
A.35 Linear trajectory with 44 beacons.	41
A.36 Linear trajectory with 48 beacons.	42
A.37 Linear trajectory with 52 beacons.	42
A.38 Linear trajectory with 56 beacons.	42
A.39 Linear trajectory with 60 beacons.	42
A.40 Linear trajectory with 64 beacons.	43

List of Tables

2.1	Comparison of common location identification technologies [5, 16, 7]	11
3.1	Table of Simulation and Forklift Parameters.	15
4.1	Table of parameters for Experiments A, B and C	26
4.2	Table of parameters for Experiments D, E and F	30
A.1	Table of parameters for all trajectories.	35

Abbreviations

AP	Access Point
AoA	Angle of Arrival
BLE	Bluetooth Low Energy
BT	Bluetooth
GPS	Global Positioning System
IPS	Indoor Positioning System
ISM	Industrial, Scientific and Medical
KF	Kalman Filter
LOS	Line-Of-Sight
MAC	Media Access Control
NIC	Network Interface Card
NLOS	Non-Line-Of-Sight
RF	Radio Frequency
RFID	Radio-Frequency Identification
RMSE	Root Mean Squared Error
RSS	Received Signal Strength
RSSI	Received Signal Strength Indicator
SIG	Special Interest Group
TDoA	Time Difference of Arrival
ToA	Time of Arrival
UHF	Ultra High Frequency
UWB	Ultra Wide Band
WiFi	Wireless Fidelity
WLAN	Wireless Local Area Network

Chapter 1

Introduction

Indoor real-time tracking systems have seen greater adoption in recent years due to the advances in technology, and the need for solutions in location-based services [5]. Some examples of these services are the inventory management of products stored in a warehouse, tracking of staff or equipment in a hospital and police or fire departments, robotics, and others [13].

One of the challenges in indoor location is to create specialized sensors for these applications, that achieve higher accuracies with low implementation costs.

Indoor Positioning Systems (IPSs) are a network of sensors and devices programmed to locate people and objects in infrastructures where the Global Positioning System (GPS) cannot be effective.

1.1 Context

This thesis is presented in the context of a tracking system for forklifts (and other indoor factory floor machinery) in a warehouse based on BLE 5.1 beacons. The beacons are placed at fixed locations in the warehouse walls, and periodically send packets with their identification.

The forklift is a moving vehicle, equipped with an antenna array that receives the beacons and can determine its position on the warehouse floor by knowing its moving speed and the relative Angles-of-Arrival of each incoming beacon. For example, if the factory has one Bluetooth beacon in each corner of a square floor, the forklift can compute its position after receiving all 4 beacons. By knowing the Angle-of-Arrival of each incoming beacon relative to its direction, the stationary position of the forklift can be determined.

However, tracking a moving object creates additional challenges. Since beacons transmit asynchronously (i.e., at different times), and since the forklift is moving, it is currently unclear which incoming beacon packet should be combined to perform the angle calculations required to determine the position of the forklift at each point in time.

1.2 Objectives

The objective of this work is to estimate the expected performance of a positioning and tracking system based on the described network topology. To do this, we developed a flexible simulator that uses real-world AoA data to track the movement of a receiver. We use this to compute the Root Mean Square Error (RMSE) of the estimated positions relative to the true positions, and explore the design space to find solutions with sub-meter accuracy.

1.3 Motivation

Unlike existing solutions like Ultra Wide Band (UWB), which are expensive and require the tracked object to be in the line of sight (LOS), Bluetooth is a solution with low implementation costs. Indoor positioning solutions via Bluetooth and Bluetooth Low Energy (BLE) have been explored in recent years. This work combines the low cost of Bluetooth with the recent advancements in antenna arrays for calculation of AoA made available in Bluetooth 5.1. relying on stationary transmitter beacons, and mobile receiver assets (i.e. the forklifts) is in itself a novel solution relative to traditional wireless location networks, where the mobile assets are typically omnidirectional transmitters.

1.4 Document structure

This thesis is organized as follows. The introduction is the first chapter and aims to help to contextualize, and to explain the motivation and the objectives for this work.

In Chapter 2, a background on the techniques to indoor positioning and a review of the most popular technologies is introduced. Also, it is presented a comparison between technologies to understand why Bluetooth-based systems are been gaining relevance in the past years.

In Chapter 3, the proposed solution to improve the current indoor positioning and indoor tracking systems is presented. It is described how the simulator is designed in order to estimate the performance of the proposed network topology based on BLE AoA.

In Chapter 4, the evaluation of the tracking performance is made. Before that, it is explained how some parameters are variable to minimize the error of the estimated position relative to the ground truth.

Chapter 5, the last chapter, presents an overview of the developed work, and it is presented the main conclusions reached given the results obtained. Suggestions for simulator improvements are also discussed in this chapter.

Chapter 2

Related Work

2.1 Background

2.1.1 Wireless indoor tracking

The tremendous growth of wireless technologies in recent years generated a high demand for accurate positioning in indoor and outdoor environments.

Different applications require different types of location information. The type discussed in this thesis is a physical location that is expressed in the form of coordinates, which identify a point on a 2D map.

Another type of indoor location is symbolic location, which is less accurate than physical, given that it only states the location with a room-level accuracy, such as on the basement, on the second floor, in the kitchen, etc [13, 3].

There are distinct topologies for positioning systems [13]. One is the remote positioning system, where the signal transmitter is mobile and a group of fixed units receives the transmitter's signal. Here, the position of the mobile unit is computed on a master station by collecting data from all fixed measuring units [13]. Another is self-positioning, where the mobile unit has the capability to compute its position. In this case, the mobile unit receives the signals transmitted from the reference points and uses their known locations to calculate its position [13].

2.1.2 Performance Metrics

Indoor positioning techniques have multiple performance criteria. The choice of the positioning technique is influenced by the tradeoff between these performance metrics in order to satisfy the application requirements.

Accuracy The accuracy of a system is the most important requirement of positioning systems and represents how close the estimated results are from a given ground truth. Usually, the root

mean squared error is adopted as the performance metric, which is the square root of the average squared distance between the estimated position and the real position. The higher the accuracy, the better the system is, however, it may be a tradeoff between accuracy and other characteristics [13, 7].

Range The transmitting range of the technology used for location estimation has a major importance. Location estimation in large spaces, such as warehouses, must have a considerable range in order to obtain better results. A higher range also results in the need for fewer reference nodes, increasing the system cost efficiency [25].

Energy Efficiency Extending the system's devices longevity is a requirement to save maintenance costs. Most sensor devices are battery-powered. Recharging the battery of these devices may sometimes not be likely, so power management is critical for these devices. Hence, this is one of the current challenges and a crucial performance metric [16].

Cost Although cost is not a performance metric, the cost of location systems should be as low as possible. The costs of a positioning system correspond to the amount of resources invested in installation and operation. They can come from many factors, such as implementation, maintenance, energy, and deployed technology.

2.1.3 Indoor location techniques

Generally, location estimation consists of three steps. First, the nodes involved in the system measure the characteristics of a signal. Second, the devices use measurements to estimate distances from fixed and mobile nodes. Finally, these measurements are combined to estimate position [3].

One of the most used position estimation techniques is triangulation. Triangulation uses the geometrical properties of triangles to estimate object location [13, 16]. Triangulation can be categorized into distance-based (lateration) or angle-based (angulation) techniques.

Lateration techniques estimate the position of a certain object by measuring its distance to multiple reference nodes. The distances can be measured based on signal attenuation or signal propagation time. Lateration can also be called multilateration as it uses range estimations from multiple reference nodes. If three reference nodes are used, then it is called trilateration. Trilateration calculates the intersection of the three circles where the mobile node is located [3]. An example of trilateration is shown in Figure 2.1.

For indoor location, using a Cartesian coordinate system is most appropriate [3]. Thus, assuming that the mobile node is located at (x, y) , the beacon 1 at (x_1, y_1) , the beacon 2 at (x_2, y_2) , and

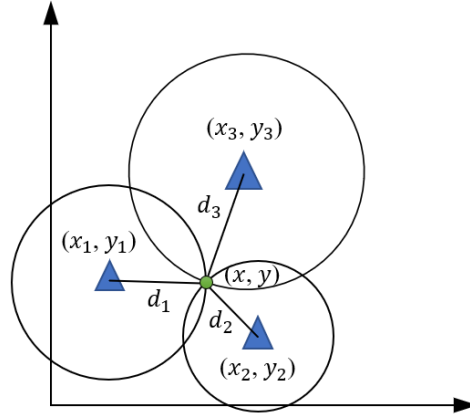


Figure 2.1: Example of trilateration with three beacons, adapted from [2].

the beacon 3 at (x_3, y_3) , the distances between each mobile node - beacon pair can be determined by the equations below [2, 21].

$$\begin{cases} d_1 = \sqrt{(x - x_1)^2 + (y - y_1)^2} \\ d_2 = \sqrt{(x - x_2)^2 + (y - y_2)^2} \\ d_3 = \sqrt{(x - x_3)^2 + (y - y_3)^2} \end{cases} \quad (2.1)$$

Assuming (x_1, y_1) as the origin point $(0, 0)$ and the distances d_1 , d_2 and d_3 are known, the equation can be simplified to

$$\begin{cases} x = \frac{d_1^2 - d_2^2 + x_2^2}{2x_2} \\ y = \frac{d_1^2 - d_3^2 - 2x_3x + y_3^2 + x_3^2}{2y_3} \end{cases} \quad (2.2)$$

This is the ideal case where the three circles intersect at one point. Due to measurement errors, getting a single intersection point is not likely, resulting in an area of intersection, or no intersection at all. In the case where the circles intersect in an area, the expected position of the mobile node is the center of the triangle formed by the three internal points. These particular cases are explained in [15].

Angulation techniques locate an object by computing the direction of the received signal, by using antenna arrays.

Both of these techniques achieve good performance in an environment with Line-of-Sight (LOS) between the transmitter and the receiver, however, the results in indoor environments, such as offices and warehouses, are worse, mainly because of the degraded signals caused by attenuation and multipath effects [11]. The multipath effect is caused when signals are mixed with some of their reflections, causing them to be noisy.

Time of Arrival Electromagnetic waves travel in the air at the speed of light. Given that the speed of light is continuous ($c = 3 \times 10^8 m/s$), the propagation time is proportional to the distance

traveled, and as such can be used to measure the distance of a receiver from a transmitter.

In ToA-based systems, the mobile device transmits a signal to at least three receiving nodes.

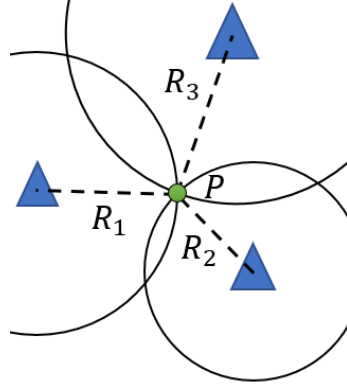


Figure 2.2: Position estimation based on ToA measurements.

The transmitted signal propagation time is measured, and the distance between the receiver and transmitter can be calculated by 2.3. This technique requires strict synchronization between all transmitters and receivers in the system, as all nodes must know about the exact transmission start time [7].

$$d = c \times \Delta t \quad (2.3)$$

To find the value of Δt the transmitted signal must be a timestamped packet.

Time Difference of Arrival Time Difference of Arrival techniques are based on the difference between propagation times of the emitted signal, measured between numerous pairs of receivers with known locations.

TDoA techniques differ from algorithms based on ToA by using the difference of arrival times instead of using the absolute arrival time. This makes the system simpler, as only the reference nodes require time synchronization since the calculation of the time difference does not need for the transmission time to be known [7, 3].

Each difference of arrival time measurement creates a hyperbole of equation 2.4.

$$L_{i,j} = \sqrt{(x_i - x)^2 + (y_i - y)^2 + (z_i - z)^2} - \sqrt{(x_j - x)^2 + (y_j - y)^2 + (z_j - z)^2} \quad (2.4)$$

where (x_i, y_i, z_i) and (x_j, y_j, z_j) are the coordinates of receivers and (x, y, z) are the mobile node coordinates.

As shown in Figure 2.3, at least three reference nodes are required. The location of the mobile node can be estimated from the intersection of the three hyperboles.

Received Signal Strength Indicator Due to its simplicity and availability, received signal strength-based methods are one of the most used in indoor location systems.

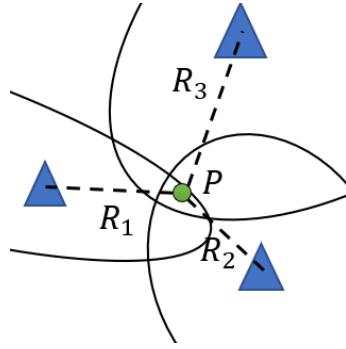


Figure 2.3: Position estimation based on TDoA measurements.

The RSS is usually measured in dBm or mW and can be used to measure the distance between the transmitter and the receiver. Using the path loss propagation model, the distance between the transmitter and the receiver can be calculated using the following formula [2, 21, 25].

$$RSSI = -10n \log_{10}(d) + A \quad (2.5)$$

where n is the signal propagation constant, and its value ranges between 2 and 4 depending on the environment; d is the distance to the transmitter, and A is the RSS at 1 meter from the transmitter. Solving for the distance:

$$d = 10^{\frac{A-RSSI}{10n}} \quad (2.6)$$

RSS-based localization requires trilateration, i.e. at least three reference nodes.

Despite RSS-based systems being simple and cost-efficient, they experience poor location accuracy, due to signal attenuation and multipath, resulting in severe RSS fluctuation [25].

Angle of Arrival In AoA, the location of the mobile node can be estimated by the intersection of angle direction lines, from at least two reference nodes to a mobile node. The combination of multiple lines places the mobile node at the intersection of those lines [3]. An example with two reference nodes is presented in Figure 2.4. More reference nodes can be used to increase accuracy [22].

Once more, using a Cartesian coordinate system, the position of the mobile node (x, y) can be calculated, assuming that the beacon 1 and 2 are at (x_1, y_1) and (x_2, y_2) respectively. The angles between the reference line and the mobile node can be determined using the equations below [1].

$$\begin{cases} \tan \theta_1 = \frac{y-y_1}{x-x_1} \\ \tan \theta_2 = \frac{y-y_2}{x-x_2} \end{cases} \quad (2.7)$$

Knowing the angles θ_1 and θ_2 , and solving to x and y , it remains

$$\begin{cases} x = \frac{x_1 \tan \theta_1 - x_2 \tan \theta_2 + y_2 - y_1}{\tan \theta_1 - \tan \theta_2} \\ y = \frac{y_1 / \tan \theta_1 - y_2 / \tan \theta_2 + x_2 - x_1}{1 / \tan \theta_1 - 1 / \tan \theta_2} \end{cases} \quad (2.8)$$

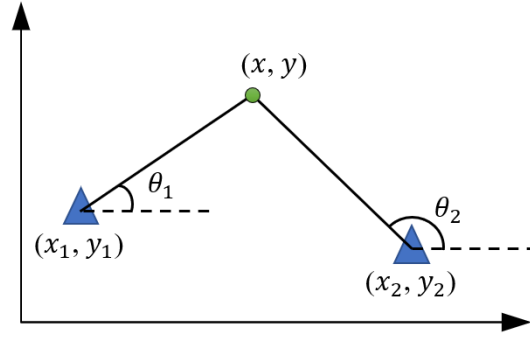


Figure 2.4: Position estimation based on AoA technique, adapted from [1]

Using more angle direction lines, it is harder to get a single intersection point. In this case, mathematical methods must be used to find the point where the mobile node is more likely to be. Some examples of mathematical methods are the least-squares intersection of lines and the nearest point to non-intersecting lines [23].

To know the angles at which the signals arrive, antenna arrays are required on the receiver, which increases implementation costs [7]. Figure 2.5 illustrates the signal receiving scenario.

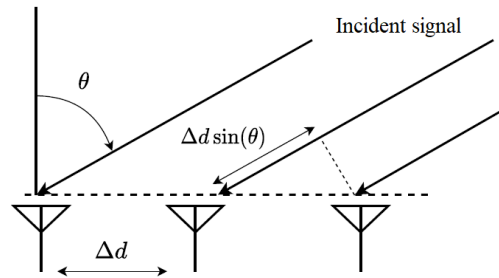


Figure 2.5: AoA based localization.

The antenna array needs to measure the phase-delay between antennas to calculate angle θ [4]. The phase-delay between signals received at a pair of adjacent antennas is given by

$$\varphi = 2\pi \left(\frac{\Delta d}{\lambda} \right) \sin \theta \quad (2.9)$$

where λ is the signal's wavelength. Solving to θ , the AoA can be found.

$$\theta = \arcsin \left(\frac{\varphi \lambda}{2\pi \Delta d} \right) \quad (2.10)$$

This technique is highly affected by the increase of the transmitter-receiver distance, multipath, and Non-Line-Of-Sight (NLOS) propagation of signals. These factors can significantly change the correct measurement of signal arrival angle. A small error in AoA calculation results in a significant error in the location estimation, degrading the accuracy of the system [7, 25].

Dead Reckoning Dead reckoning consists of estimating the current position entirely based on information from previous positions. Current positions are calculated based on the last determined position plus known or estimated speeds over a span of time. Dead reckoning is used by inertial navigation systems.

The main problem of this process is that the error is cumulative, i.e. the difference between the estimated position and the real position may grow over time [7].

2.1.4 Overview of the existing technologies

This subsection presents the state of the art in indoor wireless positioning systems that use radio frequency (RF) technologies.

GPS The global positioning system is the most popular radio navigation system and has been used worldwide for positioning in outdoor environments, such as car navigation. Nevertheless, GPS and equivalent satellite-based location systems can't be used in indoor environments because of their inability to penetrate obstacles, such as buildings, that are present in the LOS between the receiver and the satellite [2, 7, 3].

RFID Radio Frequency Identification is a wireless technology used in indoor location systems, that allows the identification of people or objects [2, 3]. The principle of RFID systems is to store and retrieve data between an RFID reader and an RFID tag, through electromagnetic transmission [8]. RFID can work on devices over several meters apart, without the need for Line-Of-Sight (LOS) propagation [7].

The RFID reader is able to read the data emitted from an RFID tag, as they use a specific protocol to communicate between each other.

RFID tags are made up of transceivers and a chip and can be classified as either active or passive [13, 16].

Active RFID tags behave like transceivers that periodically emit data along with their identification. They are equipped with a battery in their circuit, making them more expensive. Active tags operate in the UHF and microwave frequency range. They can reach more than hundreds of meters of range and are not able to achieve sub-meter accuracy, which makes them suitable for long-distance tracking positioning [13, 8, 25].

Passive RFID tags operate without a battery. Their working principle is to use the energy provided from the RFID reader, and as a result, their ranges are very limited (1 m - 5 m). They operate in the low, high, UHF, and microwave frequency range. They are much smaller and lighter and cost less than the active tags [25].

These systems are frequently used in complex indoor environments such as offices, warehouses, hospitals, etc. [8]. It has many applications like personal access control, store regulation, object tracking, logistics, etc. [3].

UWB Ultra Wide Band is one of the most accurate technologies available, providing good performance in indoor location systems. Reference [22] show that centimeter-level accuracy can be achievable using ToA techniques.

This technology is based on the transmission of ultrashort pulses with low duty-cycle, which results in reduced power consumption [16, 25].

UWB is particularly appealing for indoor localization since it is immune to interference from other signals and can penetrate walls. UWB short-duration pulses are also easy to filter, providing good robustness to multipath [25].

UWB hardware is expensive, as it is composed of a radio signal generator and multiple receivers that capture the propagated signal [7].

WiFi WiFi is the standard for wireless data transmission technology. It uses electromagnetic waves for data transmission, in the range between 2.4 GHz and 5 GHz.

In 2007, WiFi had a transmission range of about hundreds of meters, which has been increased to about 1 km [13, 25].

Most of the current smartphones, laptops, and other portable devices are WiFi-compatible. Moreover, the fact that most buildings already have an established WLAN infrastructure, makes it appealing for indoor location, as it does not require to install any additional software or hardware, and does not require LOS communication [7].

Most positioning systems based on WiFi are based on RSS measurements. As Network Interface Cards (NICs) support RSS measurements from access points within their range, there is no need for specialized hardware, which makes this type of positioning to be a cost-effective solution [7, 10].

Bluetooth Low Energy Bluetooth Low Energy was introduced in 2010 as part of the Bluetooth 4.0 specification [6]. It was designed for applications that do not require large data transfers, and desire to have high energy efficiency and low cost.

At the physical layer, BLE operates in the 2.4 GHz ISM band. It defines 40 orthogonal channels divided into 3 advertising channels that are used for device finding, connection setup, and broadcasting messages, and 37 data channels for bidirectional data exchanging between the two devices [6, 4].

The key advantage of BLE is its low energy consumption which allows the transmitters (beacons) batteries to last from months to years [11]. Other benefits of using Bluetooth-based systems are their availability, low cost of maintenance, and small size of their components [7].

Bluetooth beacons are small-sized and low-cost devices [21] that consist of an antenna, a battery to provide power supply, and a BT chipset. As they are powered by batteries, they have more portability than WiFi APs, since there is no need to connect cables to electrical outlets. Due to this portability, they can be strategically positioned around a room to maximize detection. The embedded antenna is omnidirectional.

Bluetooth beacons can reach up to 60 meters of transmission range [21], however, that results in higher energy consumption. Usually, transmissions are set to a range between 2 to 5 meters.

The BLE beacon broadcast information includes the MAC address, Universal Unique Identifier (UUID), battery level and RSSI [14].

Bluetooth beacons have a variable broadcast periodicity, as their signal is usually transmitted from a periodicity of 20 ms up to 10 seconds. Increasing the transmission period extends the beacon's battery lifetime. The time between consecutive transmissions is also known as advertising interval [21].

In the BLE 5.1 standard, the Bluetooth SIG included a direction-finding feature to determine the position of BLE beacons based on AoA estimation.

As the BLE methods that rely on RSSI do not achieve high accuracies, the addition of the direction-finding feature reforms the position finding problem [4, 20].

2.1.5 Summary

For comparison, we consider the parameters presented in 2.1.2, as they are the most commonly used to evaluate a certain technology, to develop an IPS [3].

Table 2.1: Comparison of common location identification technologies [5, 16, 7]

Technology	Accuracy	Pros	Cons
GPS	10 m - 20 m	Global scale coverage	Expensive infrastructure, only outdoor environments, very high power consumption
RFID	1 m - 5 m	Low cost, high energy efficiency	Low precision
UWB	≥ 10 cm	High accuracy, immune to interference, low power consumption	High implementation cost
WiFi	1 m - 5 m	Low cost, widely available	Prone to noise, low accuracy
Bluetooth	2 m - 5 m	Low cost, low power consumption	Prone to noise, low accuracy

2.2 Literature Review

To overcome the RSSI fluctuation on RSS-based systems, [2] uses a Kalman filter to smooth the raw RSSI values. That leads to the fluctuation of the measured values decrease significantly.

Moving receivers at high speeds require a shorter advertising interval, so this becomes a trade-off when designing the locating system. Reference [12] shows that when the receiver moves faster than 45 km/h, the absolute error can get larger than 4 meters. Moreover, the reference provides an extensive study on the relationship between position estimation accuracy, advertising interval, and object moving speed.

There are plenty of beacon suppliers in the market. Reference [21] uses the Gimbal Series 21 beacons to develop an application to enhance the user experience in a museum. These beacons have a typical battery life-time of 18 months when transmitting at an advertising interval of 100 ms. The indoor location system relies on BLE beacons' capabilities to estimate the location of the visitor, based on the RSSI technique. In addition, the system implements a Kalman filter to increase location accuracy and precision. The Kalman filter is often used for smoothing noisy data by taking a set of noisy measurements and estimating the real value of a given variable [3].

Another commercial approach is Apple's iBeacons, which were announced in 2013, that are also designed for location purposes [3, 25].

Article [14] show that a beacon with an advertising interval of 500 ms, can last up to 2 years.

BLE can be used with different location techniques, but most of the existing BLE location systems rely on trilateration techniques using the measurements of RSSI values.

Article [9] states that, as WiFi APs operate with higher transmission power, the overall RSS is higher compared with the BLE, requiring more BLE beacons to achieve similar accuracies. It also shows that the increase in the number of beacons leads to more accurate results. The results were obtained with beacons deployed on a grid topology.

However, in [19], a BLE IPS using a trilateration technique based on RSSI measurements is proposed. A set of nine beacons placed on the ceiling broadcast a signal every 400 ms carrying information, such as their identification. The mobile node collects the RSSI of the three nearest beacons and calculates the distance between itself and each of the three beacons.

Due to the fact that this is a recent technology, there is a lack of commercial hardware supporting this feature. However, [4] was one of the first to carry out an intensive study on the BLE 5.1 positioning system.

Chapter 3

Simulator

In this chapter, the proposed solution to improve the current indoor positioning and indoor tracking systems is described. The proposed solution makes use of the capabilities of the recently released Bluetooth 5.1 specification, which enables a direction-finding feature based on Angle of Arrival. The reason to adopt this technique is that it improves accuracy relatively to Bluetooth systems based on RSSI techniques while maintaining its implementation costs low, which are the main advantages of Bluetooth Low Energy protocol relative to other technologies. The improvement in accuracy happens because AoA does not have to deal with the fluctuations of the RSSI measurements.

The proposed solution is based on a network topology with fixed low-cost beacons with omnidirectional antennas, and a mobile receiver with an antenna array. The receiver reads the periodic transmissions from the beacons, and can autonomously compute its position on the map, even under beacon failing circumstances, due to the implementation of a Kalman Filter algorithm that makes predictions of the vehicle position based on its velocity measurements.

The grid of fixed beacons can scale with ease and at low cost and can be deployed in any location. The location algorithms are also scalable, which allows us to do an extensive study in this area.

3.1 Simulator Description

The main objective of the simulator is to determine the accuracy of vehicle tracking for the Bluetooth AoA scenario described previously.

The second is that the simulation tool should support the specification of multiple simulation parameters;

Consequently, we adjust the simulation parameters (i.e., number of beacons, packet processing) to optimize the positioning and tracking, i.e. to minimize the RMSE of the estimated position relative to the real position;

And finally, to evaluate the tracking performance when using the optimal parameters.

The simulator, coded in Java, allows us to get an estimation of the behavior of the algorithm in a real-world application. It also allows finding optimal parameters to extract the best performance. The parameters that the simulator can take as inputs are divided into Simulation Parameters and Forklift Parameters.

The Simulation Parameters are the number of beacons, the period of transmission of each beacon, the position of those beacons (e.g., if it's in the middle of the room, or along the perimeter), the shape, and dimensions of the respective room, and the simulation time.

The Forklift Parameters that can be given by the user are, the initial position of the forklift on the map, the type of trajectory (e.g., linear, parable, cosine, random, and others), the antenna dataset (if we want data sampled from a Gaussian antenna with a given mean and standard deviation, or from data from a real-world antenna), uncertainty used in the Kalman Filter, the minimum number of packets required to estimate the position, the estimation period, estimation strategies and packet filtering policies.

The Simulation Parameters and Forklift Parameters are described on Table 3.1.

We evaluate the performance of the Bluetooth AoA tracking by calculating the RMSE of the estimated position relative to the real position of the moving vehicle. That is given by the following formula:

$$\sqrt{\frac{1}{n} \sum_{i=1}^n (\hat{y}_i - y_i)^2} \quad (3.1)$$

The purpose of the simulator is to determine if using AoA information is enough to achieve location accuracy that is below 1 meter of error.

3.2 Simulator Architecture

This section describes how the simulator was designed to accomplish its objectives. The simulator is a timed process, so all the objects have an internal clock that advances every simulation timestep. The internal state of each object is updated according to the passage of time (e.g., the internal clock of a Beacon increase by 1 ms every simulation timestep, and creates a packet every beacon period, which then will be accepted by the forklift). The actions made by the objects are fully based on events, such as the creation of a packet and the reception of it. The main objects contained in the program are the Room, the Forklift, and the Beacons. The only event associated with the Beacon object is the creation of a packet. The events related to the Forklift object are the reading of the packets, the prediction through the Kalman Filter and Dead Reckoning technique, and the estimation of the position and the movement to the next position.

Table 3.1: Table of Simulation and Forklift Parameters.

Parameter	Variable	Description
Beacon placement	Perimeter	Places the beacons along the perimeter, or in the middle of the room
Number of beacons	PerimeterCount	Number of beacons used in the simulation, that are placed equally spaced from each other along the perimeter
Height of the room	RoomHeight	Sets the height of the room
Width of the room	RoomWidth	Sets the width of the room
Period of emission	Period	Sets the corresponding period in every beacon
Simulation time	SimTime	Sets the duration of the simulation
Type of movement	Movement	Sets the type of trajectory the forklift follows along the room
Initial position	StartPos	Sets the initial position of the forklift on the room
Period of data gathering	StatsGatherPeriod	Sets the period that the simulation stores the variables of interest (real, estimated and measured positions)
Estimation period	EstimationPeriod	Sets the period with which the forklift tries to estimate its position
Smoothness	Uncertainty	Sets the value that indicates how much the receiver relies on the measured samples
Minimum number of packets	MinPackets	Sets the minimum number of packets required for the forklift to estimate its position
Measured angle dataset	AntennaData	Samples the angles based on a hidden known real angle according to a measured angle dataset
Type of estimator	EstimationFunction	Sets the weights of the packets based on different strategies and estimates the position through the least squares method
Type of filter	PacketFilter	Defines the packet filtering policy

3.2.1 Room

The room is an object that represents the map layout. This class stores the parameters of the room's width and length to create a room of these dimensions. The room does not model obstacles, so the beacons and the forklift have LOS communication.

In the next chapter we will test two different room dimensions: a squared 10m x 10m room, and a 4m x 100m corridor.

This class also contains the list of the existing beacon and forklift objects and is responsible to place those objects in the Room and inform the forklift where the beacons are positioned in the room. This step is important because it will help the forklift to simulate the AoA of the packets sent by the beacons. The position of the beacons can be done in two ways: either by positioning the beacons along the perimeter or by putting the beacons in the middle of the room in the form of

a grid. This process is made so that the beacons are equally spaced.

3.2.2 Beacon

The beacon class models the beacon object. Beacons are simple objects which generate a packet at a given time, so the class has a method to simulate it. The internal clock of each beacon is initialized at a random value, to desynchronize the generation of packets. Each beacon has its identification for the forklift to know where the packets come from.

3.2.3 Packet

A class that represents a single Bluetooth packet transmitted by a beacon. It is generated by the Beacon class and it's given to a Forklift queue, that collects the received packets until it uses them for position estimation. After estimation, the queue is emptied.

Once the receiving process is done it turns into a ReceivedPacket object. The ReceivedPacket object extends from the Packet object, and it has attributed to it an estimated AoA and estimated RSSI. It also has a timestamp for the time of reception.

3.2.4 Forklift

The forklift class models the forklift object, therefore it's able to model its position and velocity while it follows a given path along with the map (i.e., a given ground truth). This class contains a set of parameters called ForkliftParameters referred to in one of the previous sections. These parameters are made variable so that we could study the behavior of each one and optimize the most important ones.

It also holds an antenna dataset from which to sample angles based on a hidden known real angle. This is also done parametrically, i.e. there are two datasets: one from data extracted from a real-world antenna and the other from a simple Gaussian distribution.

The antenna array used for real-world measures is presented in Figure 3.1 and it's based on the Telink TLSR8258 board. The measurements were done in two environments: in an indoor environment and an anechoic chamber. The results of the measured angles given a real angle for the indoor environment are shown in Figure 3.2. It is noticeable the presence of many outliers. The outliers result from measurement errors due to multipath propagation. This is a problem that the algorithm must deal with. As the main concentration of values remains near the median, the outliers could be filtered using a median filter.

The Gaussian antenna has a mean equal to 0 and a "configurable" standard deviation (sigma). When using the Gaussian antenna, we used a sigma of 2 degrees.

This class contains a queue with the packets that were sent by the beacons for post position estimation. In the receiving process, to simulate the reception of beacons and the calculation of AoA by the antenna array, the forklift reads the queue every simulation timestep. Note that we consider that the transmission and reception of the packet is instantaneous. If there's a packet in

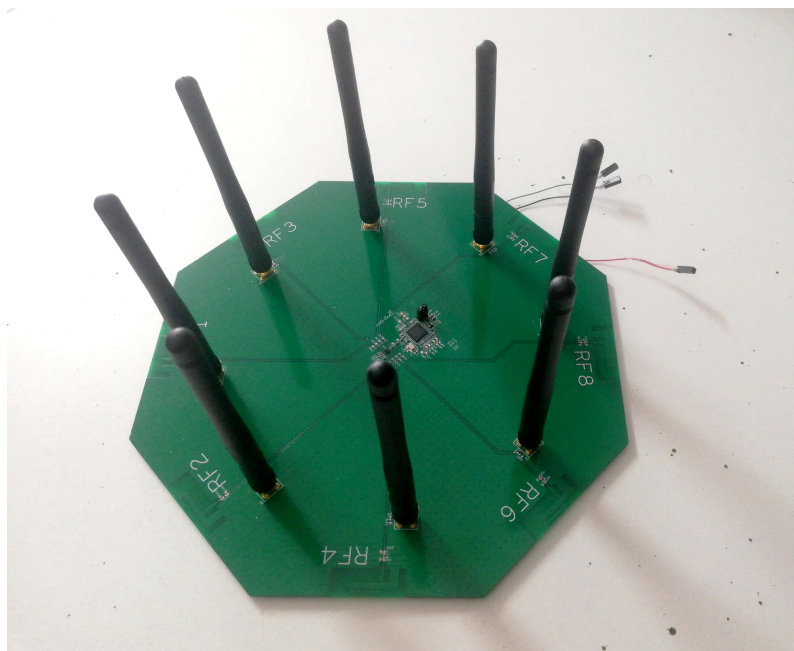


Figure 3.1: Antenna array based on the TLSR8258 [17].

the queue, the forklift can determine from which beacon the packet was originated, and which coordinates that beacon is positioned.

To calculate the real AoA in the simulation, the forklift must know its position on the map (which does not happen in the real case) and calculate the angle between the beacon and the x axis of the forklift. This was the axis we used as a reference to measure the angles.

The calculation of the angle is given by the formula 3.2. The angle is set from zero to 360 degrees.

$$AoA = \arctan\left(\frac{y_{beacon} - y_{forklift}}{x_{beacon} - x_{forklift}}\right) \quad (3.2)$$

The RSSI is estimated in this process as well. This value represents the intensity of the received signal and can be used to attribute weights to packets. In this case, we assumed a transmitted signal power of 1 W, with a frequency of 2.5 GHz (wavelength of 12 cm) and receiving and transmitting antennas with a gain of 0 dB. So, using the Friis equation, the RSSI in function of the distance of forklift to beacon in this case is provided in 3.3.

$$RSSI = 10 \log_{10} \left(\frac{0.12}{4\pi d} \right)^2 \quad (3.3)$$

After the received packets are processed, the packets go to a list of received packets. The packets on this list are consumed when the forklift tries to estimate its position. The forklift tries to estimate its position every 100 ms by default.

Before estimating its position, the forklift checks if there are enough packets in the list of received packets to do it. If so, we get the orientation of those packets based on their AoA and

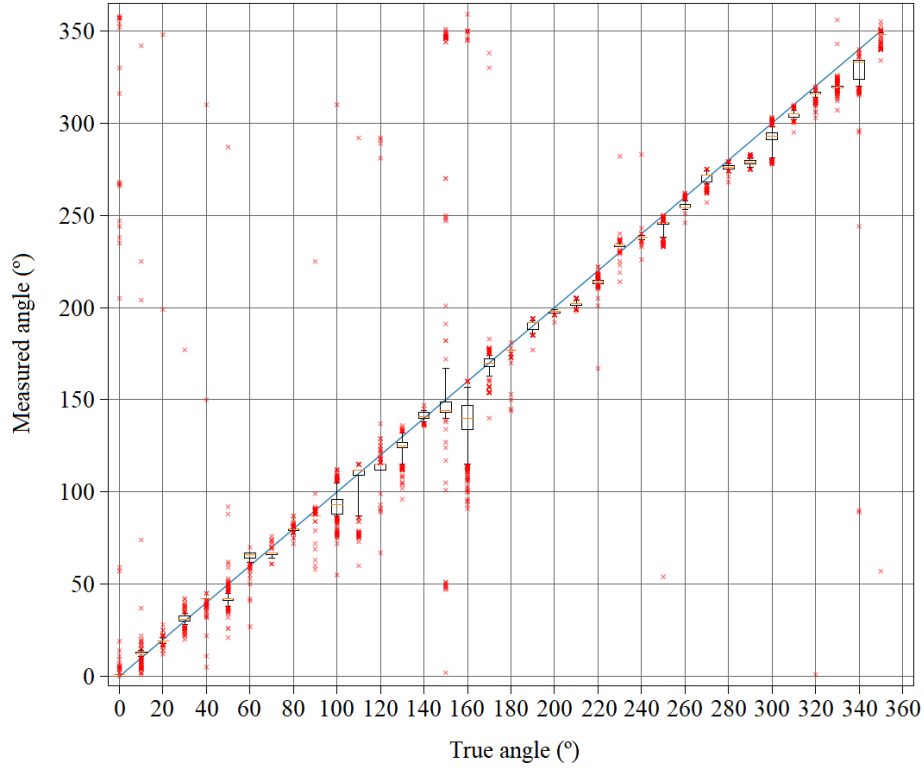


Figure 3.2: Results for a Telink kit in indoor environment [17].

then we estimate a point via the least squares method. To obtain better precision on the estimated point we use weighted least squares.

The method receives a list of the AoA (i.e., an orientation (angle) and a starting point p (beacon position) with a given weight w), with at least two direction lines.

It creates the direction vector n with magnitude 1, by calculating the cosine and the sine of the angles.

Next, creates the array of all projectors nn^T .

$$nn^T = nn^T \quad (3.4)$$

Then, the orthocomplement projectors to n

$$Imnn^T = I - nn^T \quad (3.5)$$

Then the R matrix and q vector are generated

$$R = \sum_{j=1}^K w_j (I - n_j n_j^T) \quad (3.6)$$

$$q = \sum_{j=1}^K w_j (I - n_j n_j^T) p_j \quad (3.7)$$

where K is the number of packets, p_j is the position of the beacon j and w_j is its respective weight.

Finally, we solve the least squares problem by computing the point for which the sum of distances to all lines is minimal. The deduction of these formulas can be found in [23].

An example where a point is estimated using this method is presented in Figure 3.3.

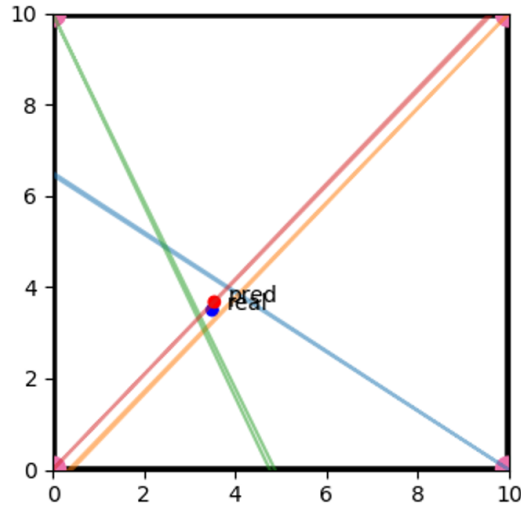


Figure 3.3: Estimated position using least squares method in comparison with real position [17].

The weighting can be done using three policies:

1. *NaiveEstimator*: All the packets have the same weight (1);
2. *EstimatorStrat1*: Packets have weights based on their estimated RSSI (0.8 - 1);
3. *EstimatorStrat2*: Packets have weights based on their reception time (0.8 - 1);

In the case of *EstimatorStrat1* and *EstimatorStrat2* the weights are calculated based on linear interpolation and are given by the formula 3.8.

$$weight = 1 + \frac{0.2}{value_{max} - value_{min}} \times (value_{sample} - value_{max}) \quad (3.8)$$

The packets that are sent to the estimator can be previously filtered or not. The objective of packet filtering is to eliminate the AoA outliers that the list of received packets might have due to the antenna dataset samples, helping to find the best value for the AoA.

In the case of when the filtering occurs, the list of received packets is separated accordingly to the beacon that they came, for each beacon, if the forklift received less than 5 packets, the filtering doesn't occur, but if there are 5 or more received packets from a certain beacon, the sublist is

filtered based on the median. If the absolute value of the difference between a packet and the median of the sub-list is greater than 2, then the packet is removed.

To smooth the samples given by the estimator, and to predict the position of the forklift between estimations, a Kalman Filter is used. `AKalmanFilter` is a class that encapsulates the Kalman Filter matrices and functions. The filter includes parameters to tune, such as the uncertainty value and the sensor error. That is useful to execute various simulations and test the best-performing parameters.

To make use of the filter, the process must be described by a linear system, which is the case of the forklift movement. The system is described by movement equations:

$$\begin{cases} p(t) = p_0 + v_0t + 0.5at^2 \\ v(t) = v_0t + at \end{cases} \quad (3.9)$$

so it can be translated to the state vector x :

$$x_{k+1} = \begin{bmatrix} p_{k+1} \\ v_{k+1} \end{bmatrix} = \begin{bmatrix} 1 & t \\ 0 & 1 \end{bmatrix} x_k + \begin{bmatrix} 0.5t^2 \\ t \end{bmatrix} a_k \quad (3.10)$$

As the forklift moves along the x and y directions, the equation 3.10 can be unfolded to:

$$x_{k+1} = \begin{bmatrix} p_{x_{k+1}} \\ p_{y_{k+1}} \\ v_{x_{k+1}} \\ v_{y_{k+1}} \end{bmatrix} = \begin{bmatrix} 1 & 0 & t & 0 \\ 0 & 1 & 0 & t \\ 0 & 0 & 1 & 0 \\ 0 & 0 & 0 & 1 \end{bmatrix} x_k + \begin{bmatrix} 0.5t^2 & 0 \\ 0 & 0.5t^2 \\ t & 0 \\ 0 & t \end{bmatrix} a_k \quad (3.11)$$

Which can be shortened to

$$x_{k+1} = Fx_k + Bu_k \quad (3.12)$$

From now on, we will treat t as dt which corresponds to the timestep of the filter, also known as the time increment. This corresponds to the period at which the filter is evaluated. Notice that we also changed the a_k to u_k to represent the control vector.

So, the F matrix corresponds to the state transition matrix:

$$F = \begin{bmatrix} 1 & 0 & dt & 0 \\ 0 & 1 & 0 & dt \\ 0 & 0 & 1 & 0 \\ 0 & 0 & 0 & 1 \end{bmatrix} \quad (3.13)$$

And the G matrix corresponds to the input matrix (maps control commands onto state changes)

$$G = \begin{bmatrix} 0.5t^2 & 0 \\ 0 & 0.5t^2 \\ t & 0 \\ 0 & t \end{bmatrix} \quad (3.14)$$

In our case we are not taking into account the acceleration so

$$u_k = \begin{bmatrix} 0 \\ 0 \end{bmatrix} \quad (3.15)$$

The measures that the forklift estimates are not only the position but also its velocity. The estimation of the velocity can be done in the forklift using a speedometer or an accelerometer, but in the simulation, it is calculated using the current estimated position and the last estimated position over their interval of time. Hence, the measure output vector y is given by the equation 3.16. The y_k is given directly to the filter.

$$y_k = \begin{bmatrix} 1 & 0 & 0 & 0 \\ 0 & 1 & 0 & 0 \\ 0 & 0 & 1 & 0 \\ 0 & 0 & 0 & 1 \end{bmatrix} x_k \quad (3.16)$$

The matrix that correlates the state vector with the measured output is the observation matrix H .

$$H = \begin{bmatrix} 1 & 0 & 0 & 0 \\ 0 & 1 & 0 & 0 \\ 0 & 0 & 1 & 0 \\ 0 & 0 & 0 & 1 \end{bmatrix} \quad (3.17)$$

Another important matrix in the filter is the Q matrix, which is the process noise covariance matrix.

$$Q = \begin{bmatrix} \sigma_x^2 & \sigma_{xy} & \sigma_{xv_x} & \sigma_{xv_y} \\ \sigma_{yx} & \sigma_y^2 & \sigma_{yv_x} & \sigma_{yv_y} \\ \sigma_{v_x x} & \sigma_{v_x y} & \sigma_{v_x}^2 & \sigma_{v_x v_y} \\ \sigma_{v_y x} & \sigma_{v_y y} & \sigma_{v_y v_x} & \sigma_{v_y}^2 \end{bmatrix} = \begin{bmatrix} dt^4/4 & 0 & dt^3/2 & 0 \\ 0 & dt^4/4 & 0 & dt^3/2 \\ dt^3/2 & 0 & dt^2 & 0 \\ 0 & dt^3/2 & 0 & dt^2 \end{bmatrix} \text{uncertainty}^2 \quad (3.18)$$

$$Q = GG^T \sigma_u^2 \quad (3.19)$$

Another matrix used in the filter calculus is the matrix R , which corresponds to the measurement noise covariance.

$$R = I\sigma_y^2 = \begin{bmatrix} 1.5 & 0 & 0 & 0 \\ 0 & 1.5 & 0 & 0 \\ 0 & 0 & 1 & 0 \\ 0 & 0 & 0 & 1 \end{bmatrix} \quad (3.20)$$

Finally, the covariance of state vector estimate matrix P .

$$P = \begin{bmatrix} 1.5 & 0 & 0 & 0 \\ 0 & 1.5 & 0 & 0 \\ 0 & 0 & 1.5 & 0 \\ 0 & 0 & 0 & 1.5 \end{bmatrix} \quad (3.21)$$

The Kalman filter works at a prediction state followed by a correction update to determine the state of the filter [18]. The prediction state estimates the current state ahead in time, while the measurement update adjusts the projected estimate with a given measurement at the current time [24].

In this case, the forklift knows where it was before (previous state), and knows how fast it is moving (state dynamics), then it can predict where it is (current state). The equations for the predict state are presented below.

priori estimate:

$$\hat{x}_{k+1} = F\hat{x}_k + Bu = F\hat{x}_k \quad (3.22)$$

The priori estimate covariance is also recalculated

$$P_k = FP_{k-1}F^T + Q \quad (3.23)$$

When the forklift successfully estimates a new position, the filter does the measurement update. Here the Kalman gain factor is calculated by

$$K_k = P_k H^T S^{-1} \quad (3.24)$$

where S is the innovation co-variance

$$S = HP_k H^T + R \quad (3.25)$$

The system state is now updated also

posteriori estimate

$$x_k = \hat{x}_k + K_k I \quad (3.26)$$

where I is the innovation matrix:

$$I = y_k - H\hat{x}_k \quad (3.27)$$

posteriori covariance

$$P_k = (I_4 - K_k H) P_k \quad (3.28)$$

The movement of the forklift is simulated by parametric functions that directly give the position x and y values in function of the time. Alternatively, it could be inertial measurements, such as velocity or acceleration as a function of time, which is not the case. The movement event is called

every simulation time step (i.e., 1 ms) and it sets a new position for the forklift, making it follow a certain trajectory. There are different types of trajectories available, such as linear, parabolic, and sinusoidal.

The flow of the whole system is described in the Figure [3.4](#).

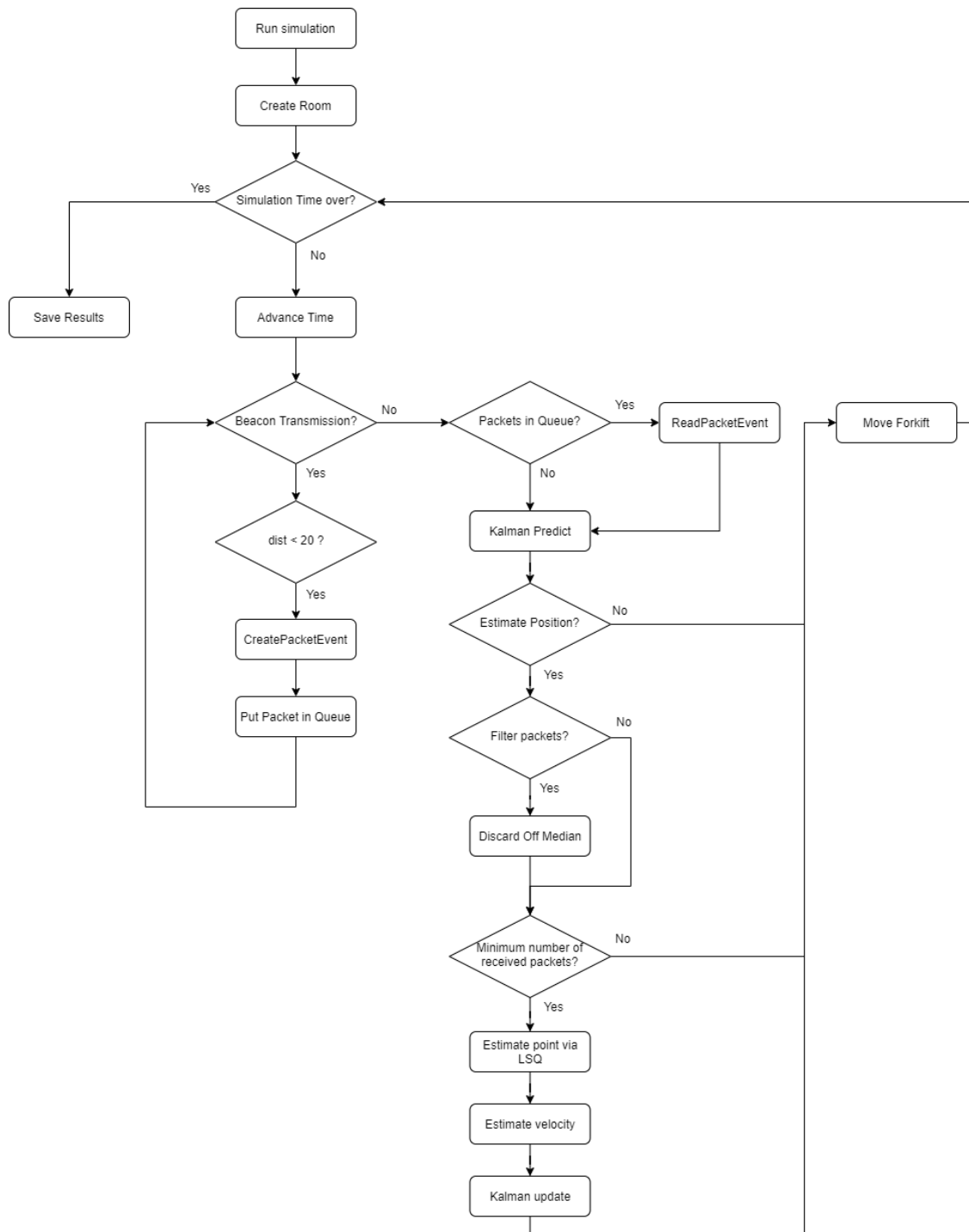


Figure 3.4: Flowchart of the system.

Chapter 4

Results

4.1 Experimental Setup

In order to evaluate the tracking performance, some simulation parameters and forklift parameters are variable. This allows us to make some conclusions on what values some parameters must have, and what is the tracking performance with those respective values. The variable parameters were already described in Table 3.1.

Prior to the evaluation of the tracking performance, three experiments were made in order to find the optimal values for the Kalman smoothness and for the number of packets required for the forklift to estimate its position. The methodology to find the optimal values was to vary the parameters referred to find the ones that result in a lower RMSE of the estimated position relative to the real position of the forklift. The values of these parameters will be used in other experiments, allowing to minimize the error in the position estimation. The sweeps were made for different beacon periods so that we could find the maximum beacon period that would give an accuracy close to the sub-meter. By extending the beacon period the beacon's battery life is extended. The values of each parameter in each experiment are listed in Table 4.1.

The trajectory used in the three experiments was sinusoidal. This trajectory was chosen because allows us to verify the behavior on complex trajectories with multiple direction changes. Also, if the tracking presents a good accuracy in this assessment, it will present better accuracies in simpler trajectories.

4.2 Defining the Uncertainty value

4.2.1 Experiment A: Uncertainty vs. Beacon Period

Firstly, we evaluated the effect of the Kalman Filter smoothing parameter (uncertainty) on the RMSE of the estimated position relative to the real position. As described in Table 3.1, the uncertainty is a value that indicates how much the receiver relies on the measured samples. If samples are noisy, the filter must have a lower uncertainty, that is, higher confidence in its internal inertial model. So, in a noisy environment, which is the case, to get better performance, the filter must

Table 4.1: Table of parameters for Experiments A, B and C¹

Variable	Value in Experiment A	Value in Experiment B	Value in Experiment C
PerimeterCount	64	16 - 64	64
RoomHeight	4 m	4 m	4 m
RoomWidth	100 m	100 m	100 m
<i>bp</i>	250 - 1000 ms	500 ms	100 - 1000 ms
SimTime	34301 ms	34301 ms	34301 ms
Movement	Cosine	Cosine	Cosine
StartPos	x = 1 m, y = 2 m	x = 1 m, y = 2 m	x = 1 m, y = 2 m
StatsGatherPeriod	1 ms	1 ms	1 ms
EstimationPeriod	10 ms	10 ms	10 ms
Uncertainty	0.01 m - 2.51 m	0.36 m	0.36 m
MinPackets	6	5-10	5-20
AntennaData	Telink	Telink	Telink
EstimationFunction	EstimatorStrat1	EstimatorStrat1	EstimatorStrat1
PacketFilter	discardOffMedian	discardOffMedian	discardOffMedian

have a lower uncertainty because there are too many erratic samples. To confirm this, a sweep of this parameter was made for various beacon periods. The results are shown in Figure 4.1.

The graph shown in Figure 4.1 shows that the RMSE increases with the increase of the uncertainty, which is expected since higher uncertainty values make the filter rely more on the samples. As the samples come from the noisy values of the antenna dataset, the higher the error relative to the ground truth. The maximum beacon period that allows us to have sub-meter accuracy is a beacon period of 500 ms, and the uncertainty that minimizes the RMSE of the estimated position relative to the real position for a beacon period of 500 ms is 0.36 m. This is the value used in the following experiments. A beacon period of 500 ms is chosen to extend the beacon's battery lifetime [14]. An uncertainty of 0.36 m, given that it's a parameter from the Kalman Filter, doesn't affect the system costs.

4.3 Defining the Minimum Number of Packets

Next, the dependency on the optimal number of packets required for the forklift to estimate its position was investigated. In the previous experiment, the value of this parameter was set to the default value, which is 6. The dependency on the minimum number of packets was taken into account because there is a trade-off between the number of packets and the age of the packets (i.e., the time passed after the forklift received the packet) that are used in the position estimation. For example, trying to estimate the position in a noisy environment (antenna data) with a low number of packets may result in an incorrect estimation; the same occurs when the estimator waits for a certain number of packets, making the first received packets old, resulting in position estimations that are computed using packets received at different real positions. This is worsened as the vehicle

¹Values in bold correspond to the ones that were varied in each experiment.

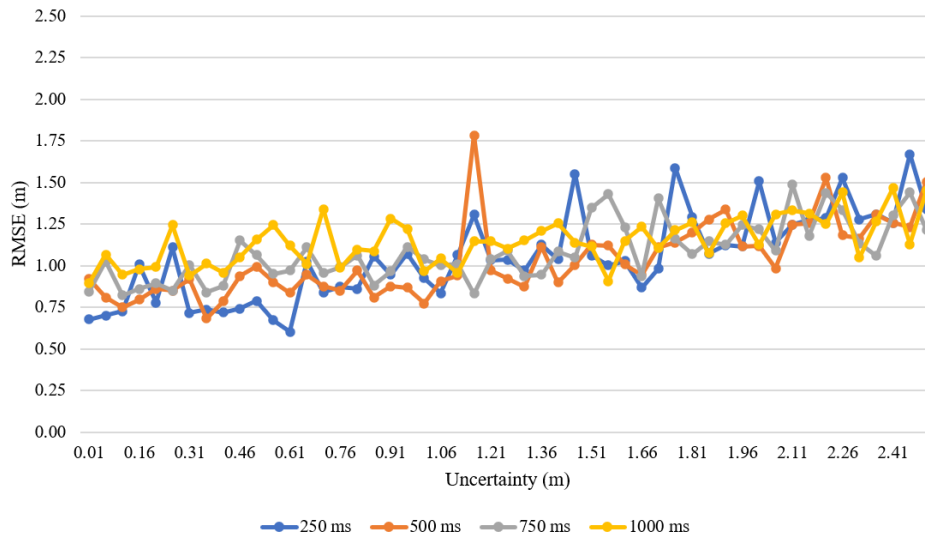


Figure 4.1: Sweep of the Kalman uncertainty.

speed increases. Previously we considered the minimum number of packets to be 6, because it is a small value which makes that the forklift does not have to wait too much to estimate its position, but in this section, we will demonstrate that this value minimizes the RMSE, under the given conditions.

4.3.1 Experiment B: Minimum Number of Packets vs. Number of Beacons

First, a sweep of this parameter was made for a different number of beacons. This allows us to check if there's any dependence between these two parameters. The results are shown in Figure 4.2.

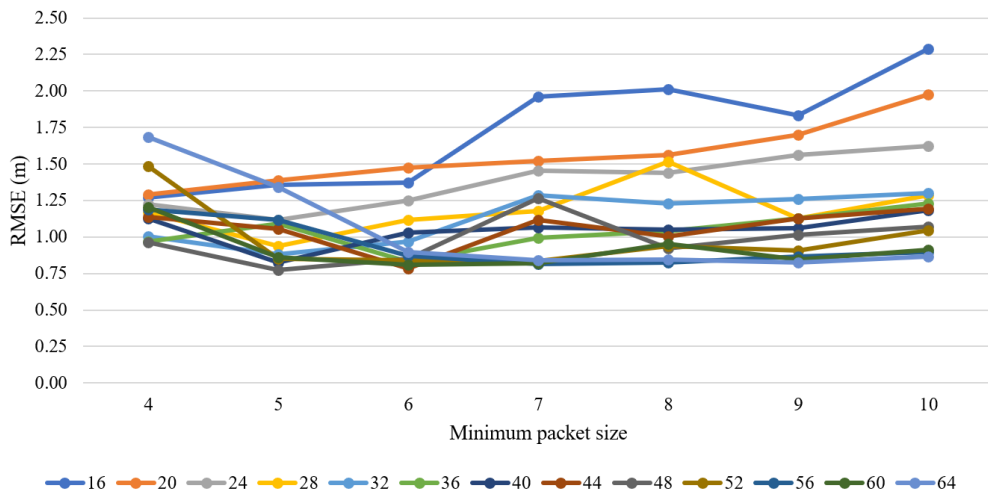


Figure 4.2: Minimum packet size sweep for different number of beacons.

Looking at the results, we can conclude that the minimum packet count does not depend on the number of beacons, as the value which minimizes the RMSE of the estimated position relative to the real position is between 5 and 6 packets, in most of the configurations. This happens, because adding more beacons increases beacon density, causing the forklift to consume the packets faster. So a solution to improve accuracy, in this case, is to vary the beacon period of the beacons rather than increase the number of beacons, which is done in the next subsection.

4.3.2 Experiment C: Minimum Number of Packets vs. Beacon Period

Knowing that the optimal value does not depend on the number of beacons, a study for the minimum number of packets with different beacon periods was made, obtaining the results shown in Figure 4.3.

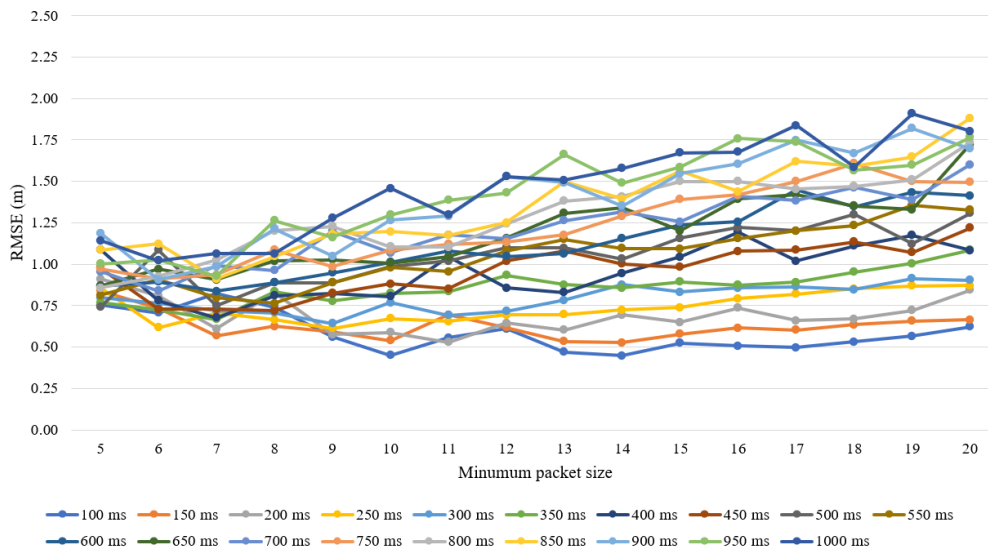


Figure 4.3: Minimum packet size sweep for different beacon periods.

Figure 4.3 shows that the minimum RMSE of the estimated position relative to the real position depends on the beacon period. Unlike the previous experiment, a decrease in the beacon period results in more packets read by the forklift per period of time. The lower the advertising interval, the better the accuracy, however, the beacon's battery life needs to be taken into account.

The graphic in Figure 4.4 shows the optimal minimum packet value for each beacon period. Analyzing the curve of minimum packet size in function of the beacon period, an approximation using a logarithmic regression can be made. The curve of approximation using logarithmic regression is also presented in Figure 4.4. It is defined by equation 4.1.

$$MinPackets = -3.272 \ln \left(\frac{bp - 50}{50} \right) + 14.301 \quad (4.1)$$

Equation 4.1 was implemented in the code to automatically define the optimal minimum packet size for a given beacon period. The result is rounded up to achieve an integer number of packets.

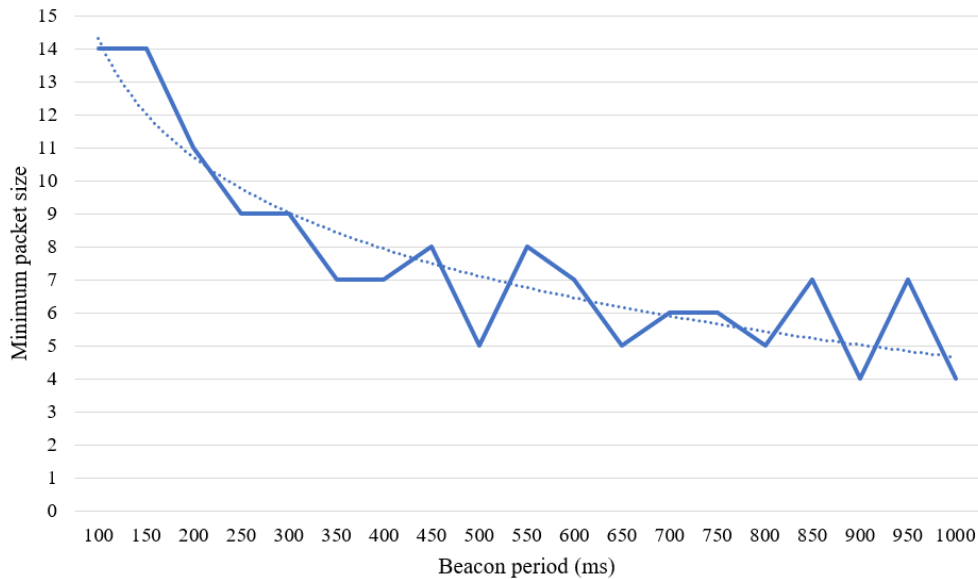


Figure 4.4: Logarithmic regression of minimum packet dependency on beacon period

As we set the beacon period parameter to 500 ms, using the formula we get an optimal minimum packet count of 7, which is used in the following experiments.

4.4 Evaluation of tracking performance

In the previous sections, we determined the values for the uncertainty, for the minimum number of packets required for the vehicle to estimate its position, and for the beacon transmission periodicity that minimized the RMSE of the estimated position relative to the real position of vehicle tracking for a cosine trajectory in a 100-meter long corridor.

In this section, we use those experimentally determined values for additional experiments. The experiments correspond to the evaluation of tracking performance under different trajectories.

Other than evaluating the tracking performance for additional trajectories, different estimation and packet filtering policies are also studied. We evaluate the tracking performance as a function of the number of beacons. We use the same 100-meter corridor and an additional square room with 10 meters of width and length. The parameters of those experiments are summarized in Table 4.2. It's also important to refer that the velocity of the forklift in these trajectories was always around 10 km/h. In general, this is considered an acceptable speed limit in indoor environments where pedestrians coexist frequently.

The objective of these experiments was to check the tracking performance for every pair filter-estimator, as well as to find the minimum number of beacons necessary to achieve sub-meter accuracy.

Table 4.2: Table of parameters for Experiments D, E and F

Variable	Value in Experiment D	Value in Experiment E	Value in Experiment F
PerimeterCount	16 - 64	16 - 64	16 - 64
RoomHeight	4 m	10 m	10 m
RoomWidth	100 m	10 m	10 m
bp	500 ms	500 ms	500 ms
SimTime	34301 ms	3201 ms	4001 ms
Movement	Cosine	Parabola	Linear
StartPos	$x = 1 \text{ m}, y = 2 \text{ m}$	$x = 0.5 \text{ m}, y = 1 \text{ m}$	$x = 1 \text{ m}, y = 1 \text{ m}$
StatsGatherPeriod	1 ms	1 ms	1 ms
EstimationPeriod	10 ms	10 ms	10 ms
Uncertainty	0.36 m	0.36 m	0.36 m
MinPackets	7	7	7
AntennaData	Telink	Telink	Telink

4.4.1 Experiment D: Tracking Evaluation on a Sinusoidal Trajectory

In Experiment D, the forklift follows a sinusoidal trajectory along a corridor 100 meter long. That allow us to verify the behavior on the same complex trajectories of previous experiences. The performance of this experiment for multiple estimation and packet filtering policies is shown in Figure 4.5.

As expected, the RMSE of the estimated position relative to the real position decreases with the increase in the number of beacons. This happens because as there are more beacons along the walls, there are also more beacons within the forklift's range, allowing it to receive more packets and to estimate its position more precisely.

However, all policies seem to have similar results, which concludes that there is no significant increase in accuracy by filtering the packets or by giving different weights to the packets. This can be justified by the fact that, as the minimum number of packets is 7, the forklift estimates its position with a low amount of packets and the weights are always similar.

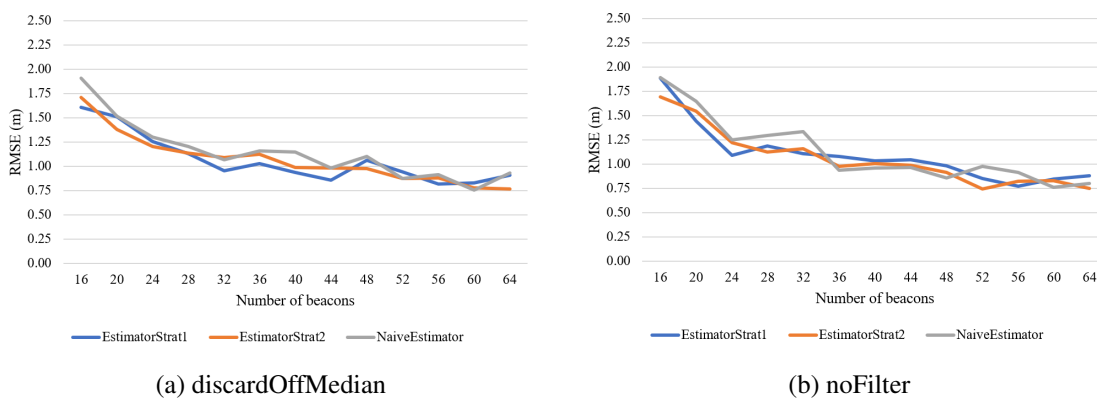


Figure 4.5: Tracking performance on Experiment D.

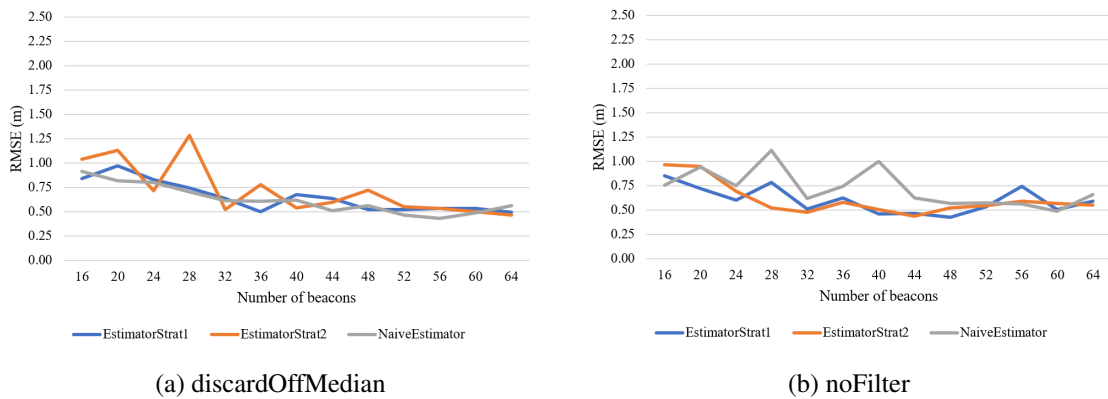


Figure 4.6: Tracking performance on Experiment E

The majority of the tracking experiments only need 50 beacons to achieve sub-meter accuracy.

4.4.2 Experiment E: Tracking Evaluation on a Parabolic Trajectory

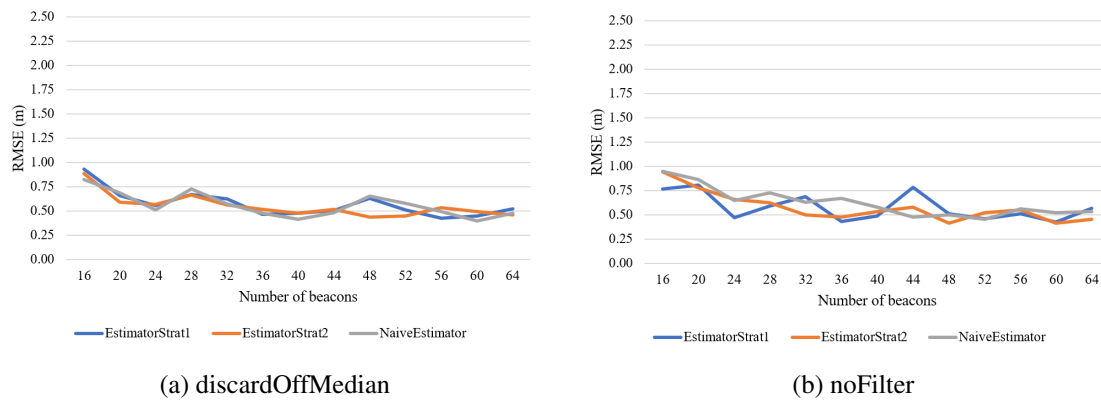
On Experiment E the forklift follows a parabolic curve crossing the room from one corner to the opposite corner. In this particular trajectory, the vehicle moves with negative acceleration, starting with a velocity higher than 10 km/h. The performance of this experiment is shown in Figure 4.6.

This trajectory presents a significant decrease in the RMSE of the estimated position relative to the real position. This happens mainly because of the higher smoothness of the trajectory compared with the sinusoidal trajectory. As it can be seen in the trajectories shown in the appendix A, the main source of error in this experiment is at the start of the trajectory where the vehicle moves at higher speeds, leading to an incorrect prediction of the Kalman Filter. In this case, sub-meter accuracy can be achieved with only 32 beacons.

4.4.3 Experiment F: Tracking Evaluation on a Linear Trajectory

In Experiment F the forklift goes through a straight line crossing the room from one corner to the other. It helps us to verify the behavior on simpler trajectories with constant speeds. The performance of this experiment is shown in Figure 4.7.

This is the simplest trajectory so the estimation error is under 1 m even for a reduced number of beacons. Also adding more beacons doesn't improve the performance by a lot as the RMSE of the estimated position relative to the real position is always about half a meter. This happens because of the linearity of the trajectory. Even with noisy estimation measurements, the forklift trajectory can be well predicted by the Kalman Filter, using inertial measurements.



(a) discardOffMedian

(b) noFilter

Figure 4.7: Tracking performance on Experiment F

Chapter 5

Conclusions and Future Work

5.1 Conclusions

In this thesis, we explored the Bluetooth Angle of Arrival capabilities in indoor positioning and indoor tracking applications, using a simulator based on empirical samples retrieved from a commercial Bluetooth Low Energy 5.1 solution. This can be useful in many ways, as it can change how the current solutions are implemented.

First, we started by exploring the current technologies and which techniques they rely on, to understand why Bluetooth-based systems are so popular and have been gaining importance in the past years. Some of the reasons for that are the high energy efficiency, low implementation costs, and high portability due to the embedded battery and small-sized components.

Then, we explained how the simulator was designed in order to accomplish multiple objectives, such as to determine the accuracy of indoor vehicle tracking based on Bluetooth Low Energy AoA, support the specification of multiple adjustable simulation parameters to minimize the RMSE of the estimated position relative to the real position and analyze the tracking performance.

The tracking performance evaluation was made in multiple scenarios, with layouts similar to the ones presented in real warehouses. The values for the RMSE of the estimated position relative to the real position obtained in the results are about 1 meter, which is what we wished to achieve. This was obtained with a beacon periodicity of 500 ms.

We observed that different packet policies give similar results. This can be justified because, as the number of packets is low, there are never enough packets to filter, and these are never old enough for the weights to take effect.

The main source of error was the computed AoA after being sampled by the antenna dataset. This happens, due to the performance of the array in an indoor environment shown in Figure 3.2.

However, it was shown that sub-meter accuracy can be achieved with a small amount of beacons that make use of AoA data to compute positions. Although AoA approaches existed prior

to Bluetooth 5.1, we have explored a novel network topology. This approach of many fixed low-cost beacons for location estimation of a small number of receivers only becomes possible by combining the characteristics of AoA with the cost profile of Bluetooth devices.

This result for the accuracy is an upgrade over the current Bluetooth systems that rely on the RSSI measurements while keeping the advantages that Bluetooth systems have relative to other technologies.

5.2 Future Work

In this thesis, a solution based on Bluetooth Angle of Arrival was proposed and simulated.

In order to compare the simulation results with a real-world application, future work includes implementing the estimation algorithms based on the least squares method on a real device and compare its performances with the simulation's.

The solutions space is extensive, and there's a lot of combinations of parameters that were not studied, that may improve the solutions. Such as trying with different rooms, different trajectories, or different velocities, etc. Those studies can be done in future work.

To improve the simulation, the effects of reflections and objects need to be considered, as well as packet losses.

Implementing a method to calculate the energy consumption and battery lifespan is also welcomed.

Appendix A

Trajectory

The following images represent the trajectories in each scenario. The parameters of the simulation are presented in Table A.1.

Table A.1: Table of parameters for all trajectories.

Variable	Value
AntennaData	Telink
EstimatonFunction	EstimatorStrat1
PacketFilter	discardOffMedian

The sinusoidal trajectory is made along a 4m x 100m corridor, while the other scenarios are made in a 10 m x 10 m room. Images are scaled.

The sequence of images allows us to see the progression of the tracking performance with the increase of the number of beacons. The label of the figures is

- Beacon
- Groundtruth
- Predicted position
- Estimated position

Figure A.1: Label of the figures.

A.1 Trajectories



Figure A.2: Sinusoidal trajectory with 16 beacons.

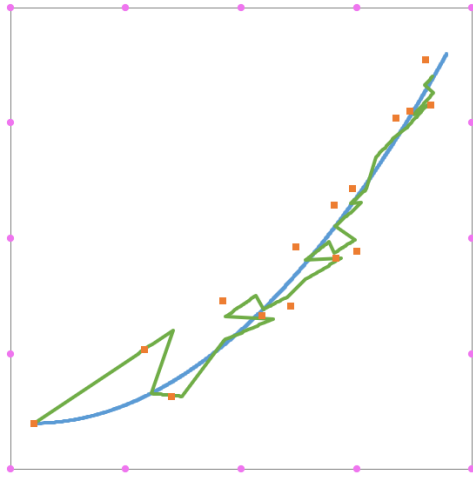


Figure A.15: Parabolic trajectory with 16 beacons.

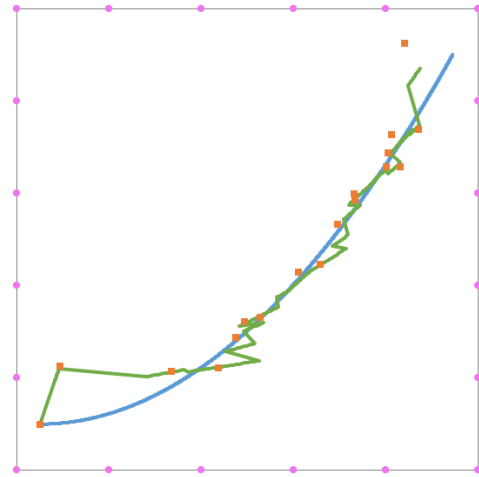


Figure A.16: Parabolic trajectory with 20 beacons.

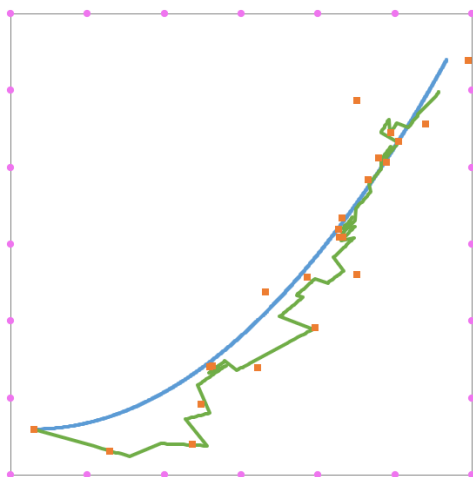


Figure A.17: Parabolic trajectory with 24 beacons.

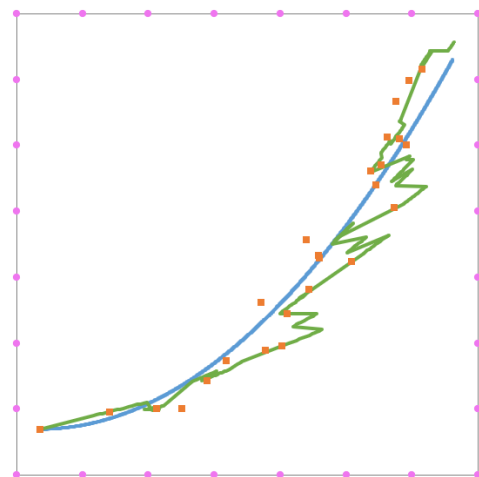


Figure A.18: Parabolic trajectory with 28 beacons.

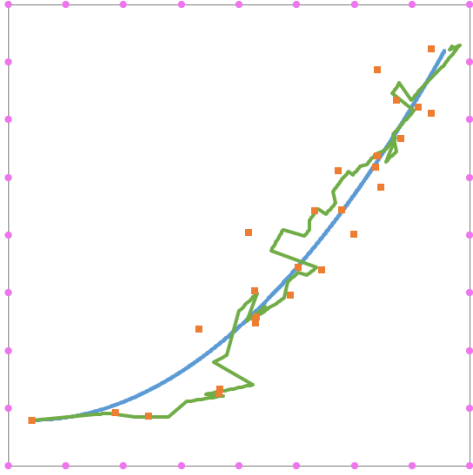


Figure A.19: Parabolic trajectory with 32 beacons.

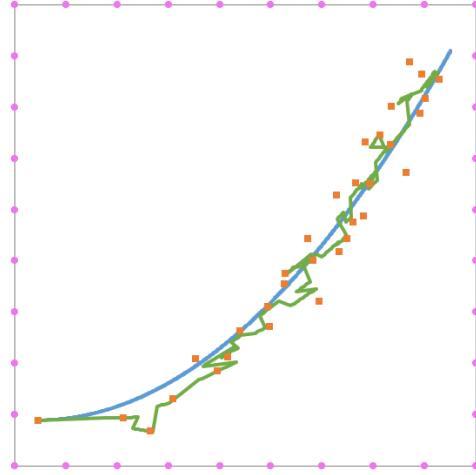


Figure A.20: Parabolic trajectory with 36 beacons.

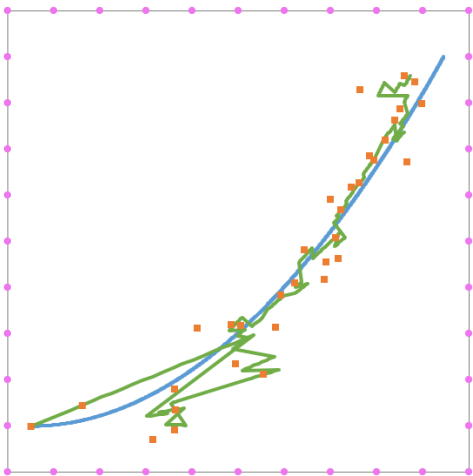


Figure A.21: Parabolic trajectory with 40 beacons.

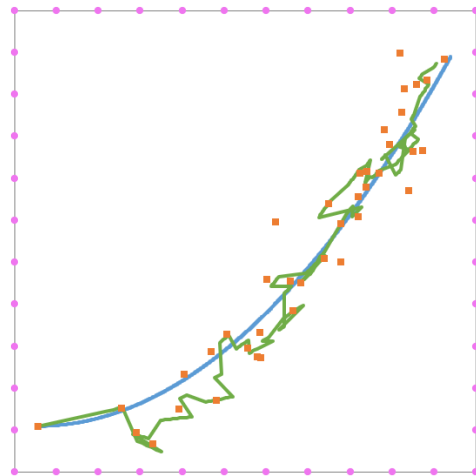


Figure A.22: Parabolic trajectory with 44 beacons.

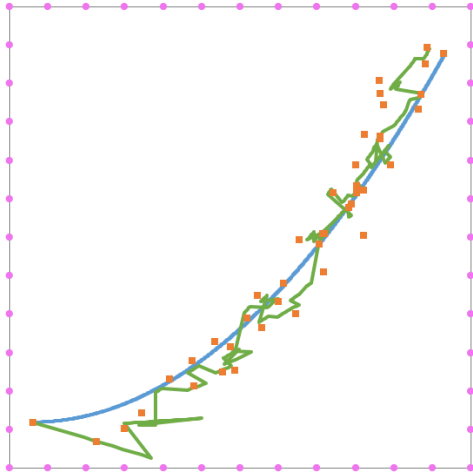


Figure A.23: Parabolic trajectory with 48 beacons.

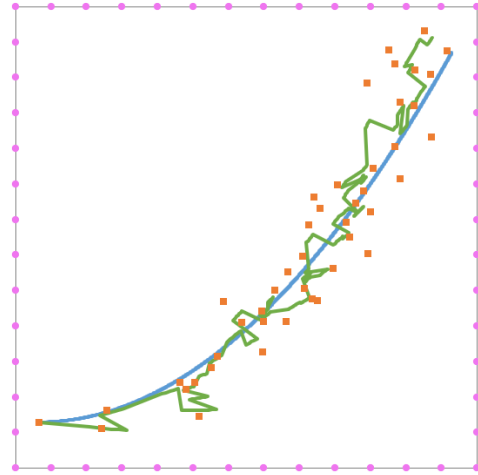


Figure A.24: Parabolic trajectory with 52 beacons.

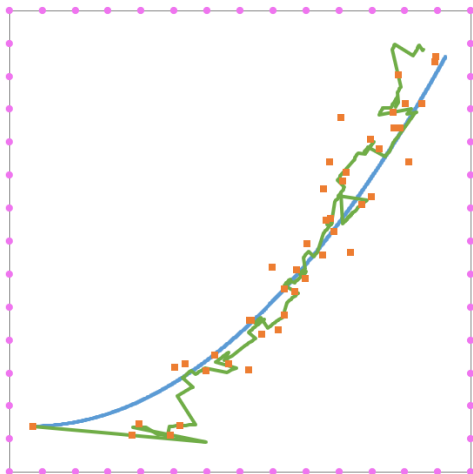


Figure A.25: Parabolic trajectory with 56 beacons.

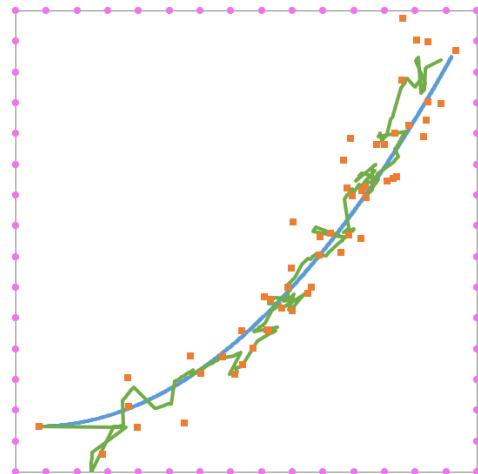


Figure A.26: Parabolic trajectory with 60 beacons.

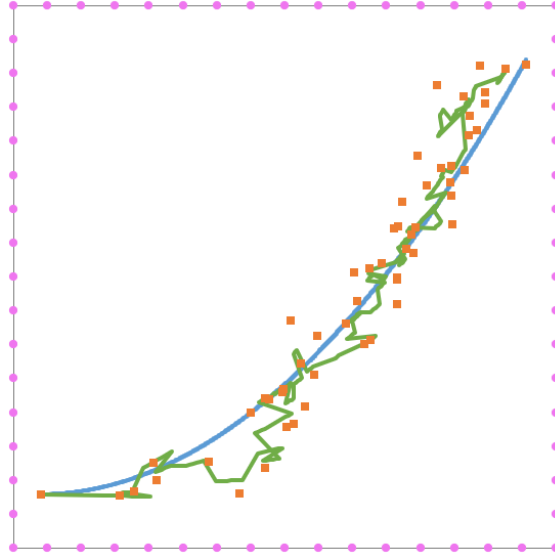


Figure A.27: Parabolic trajectory with 64 beacons.

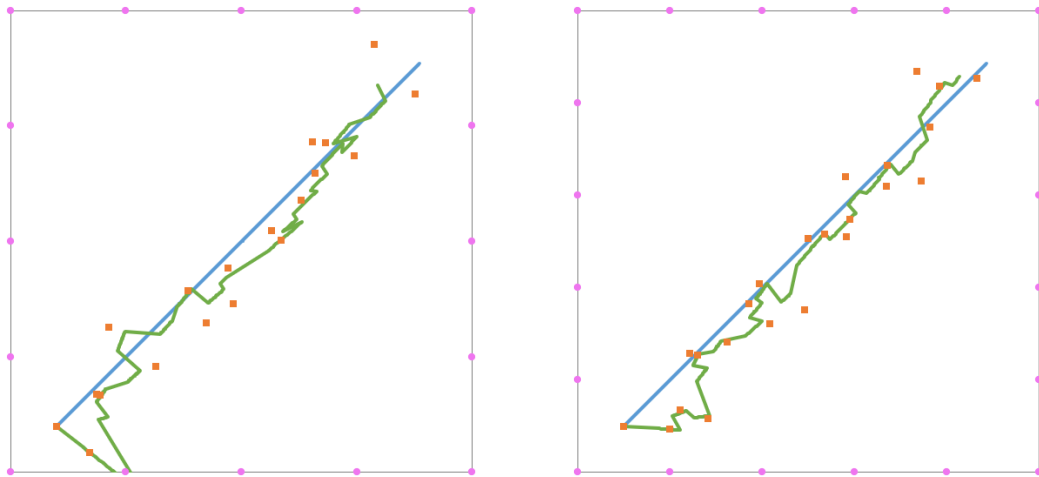


Figure A.28: Linear trajectory with 16 beacons. Figure A.29: Linear trajectory with 20 beacons.

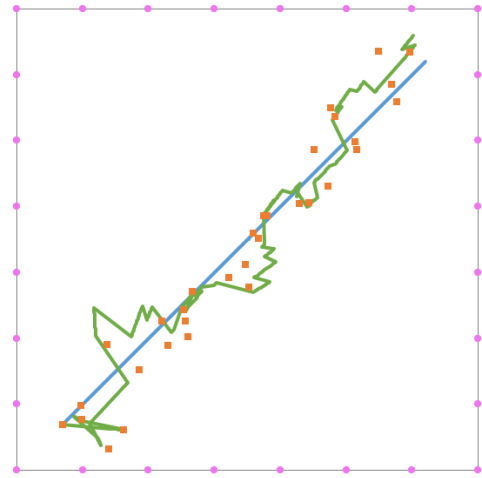
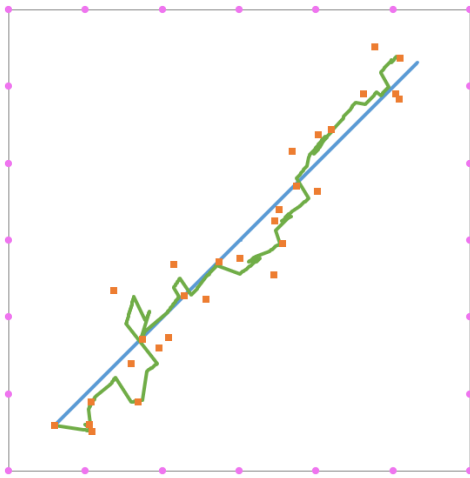


Figure A.30: Linear trajectory with 24 beacons. Figure A.31: Linear trajectory with 28 beacons.

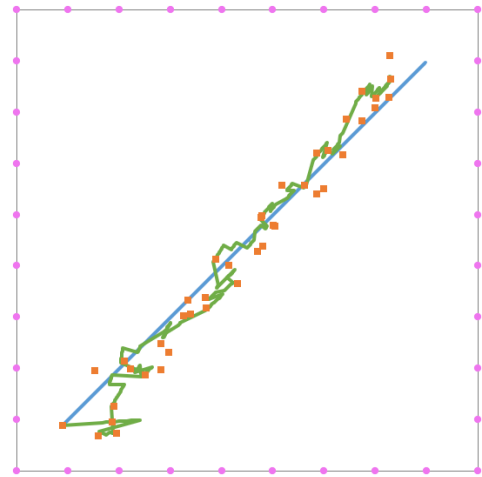
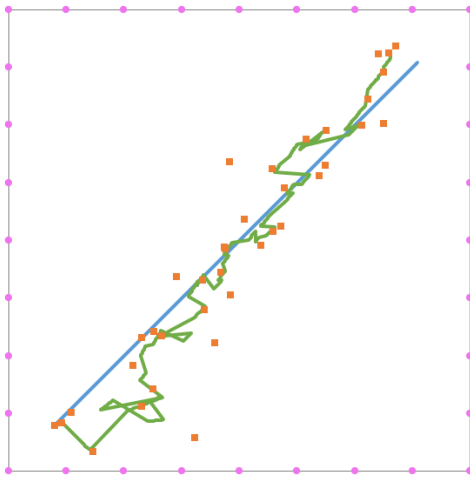


Figure A.32: Linear trajectory with 32 beacons. Figure A.33: Linear trajectory with 36 beacons.

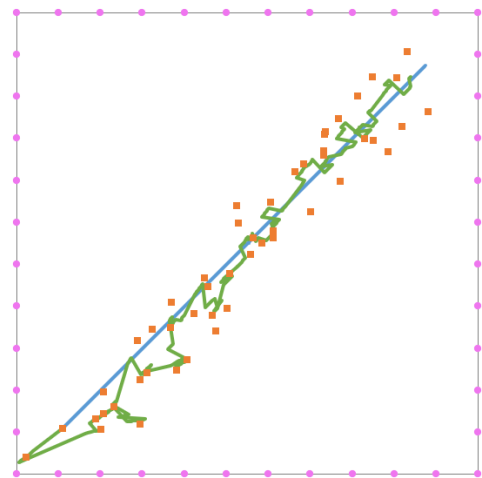
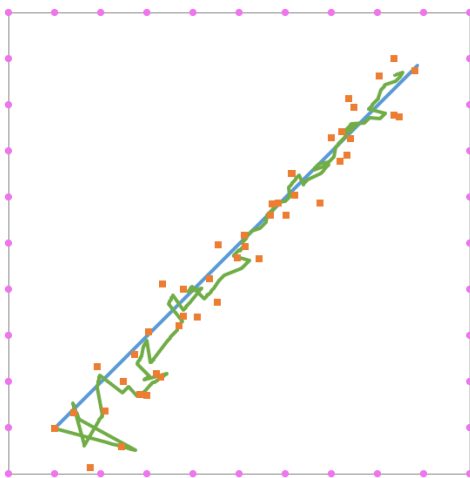


Figure A.34: Linear trajectory with 40 beacons. Figure A.35: Linear trajectory with 44 beacons.

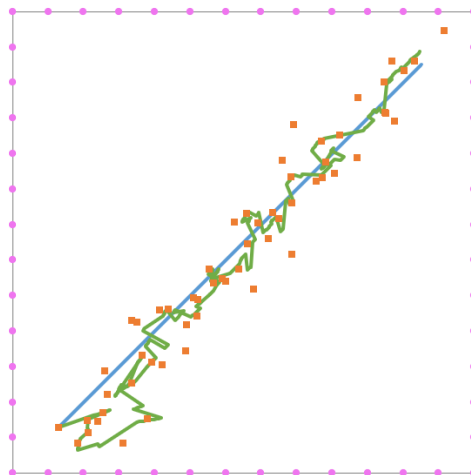
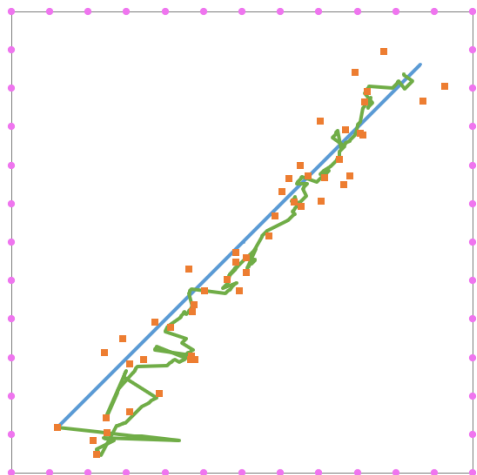


Figure A.36: Linear trajectory with 48 beacons. Figure A.37: Linear trajectory with 52 beacons.

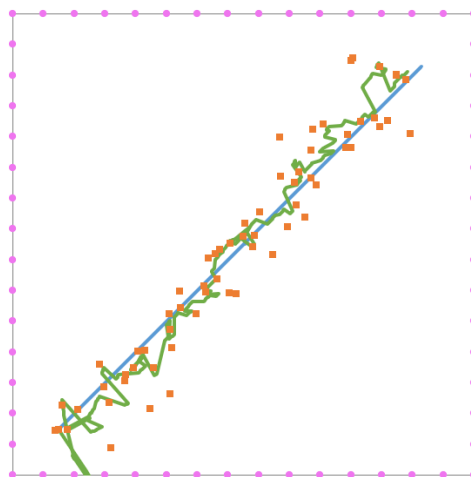
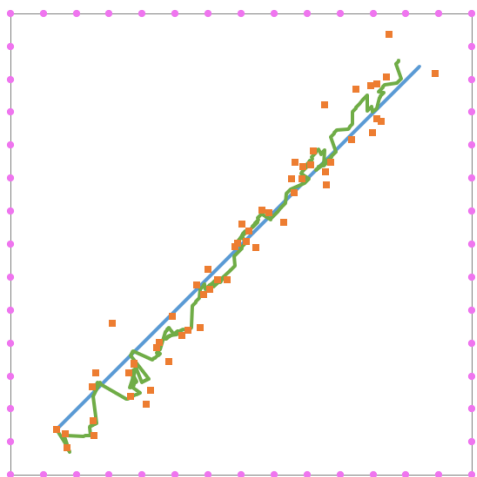


Figure A.38: Linear trajectory with 56 beacons. Figure A.39: Linear trajectory with 60 beacons.

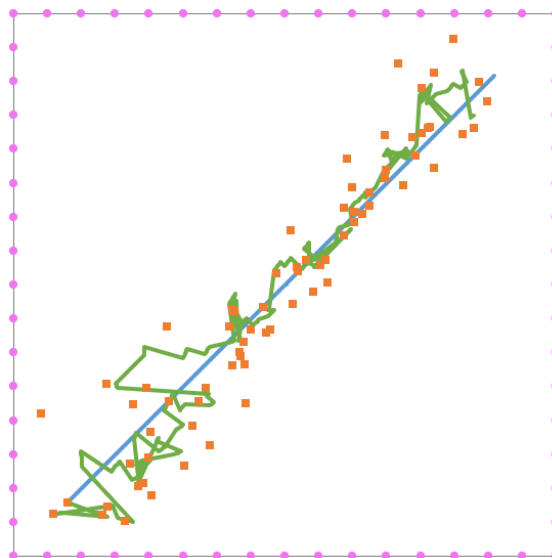


Figure A.40: Linear trajectory with 64 beacons.

References

- [1] A. Alexandrov and V. Monov. *Method for Indoor Localization of Mobile Devices Based on AoA and Kalman Filtering*, pages 1–12. Springer International Publishing, 2019.
- [2] L. Bai, F. Ciravegna, R. Bond, and M. Mulvenna. A low cost indoor positioning system using bluetooth low energy. *IEEE Access*, 8:136858–136871, 2020.
- [3] Ramon Brena, Juan García-Vázquez, Carlos Galván Tejada, D. Munoz, Cesar Vargas-Rosales, James Fangmeyer Jr, and Alberto Palma. Evolution of indoor positioning technologies: A survey. *Journal of Sensors*, 2017, 03 2017.
- [4] Marco Cominelli, Paul Patras, and Francesco Gringoli. Dead on arrival: An empirical study of the bluetooth 5.1 positioning system. In *Proceedings of the 13th International Workshop on Wireless Network Testbeds, Experimental Evaluation & Characterization*, pages 13–20, 10 2019.
- [5] D. Dardari, P. Closas, and P. M. Djurić. Indoor tracking: Theory, methods, and technologies. *IEEE Transactions on Vehicular Technology*, 64:1263–1278, 04 2015.
- [6] Seyed Mahdi Darroudi and Carles Gomez. Bluetooth low energy mesh networks: A survey. *Sensors*, 17, 06 2017.
- [7] Zahid Farid, Rosdiadee Nordin, and Mahamod Ismail. Recent advances in wireless indoor localization techniques and system. *Journal of Computer Networks and Communications*, 2013, 09 2013.
- [8] Y. Gu, A. Lo, and I. Niemegeers. A survey of indoor positioning systems for wireless personal networks. *IEEE Communications Surveys Tutorials*, 11(1):13–32, 2009.
- [9] M. Ji, J. Kim, J. Jeon, and Y. Cho. Analysis of positioning accuracy corresponding to the number of ble beacons in indoor positioning system. In *2015 17th International Conference on Advanced Communication Technology (ICACT)*, pages 92–95, 2015.
- [10] K. Kaemarungsi and P. Krishnamurthy. Properties of indoor received signal strength for wlan location fingerprinting. In *The First Annual International Conference on Mobile and Ubiquitous Systems: Networking and Services, 2004. MOBIQUITOUS 2004.*, pages 14–23, 2004.
- [11] Pavel Kriz, Filip Maly, and Kozel Tomáš. Improving indoor localization using bluetooth low energy beacons. *Mobile Information Systems*, 2016:1–11, 04 2016.
- [12] C. H. Lam and J. She. Distance estimation on moving object using ble beacon. In *2019 International Conference on Wireless and Mobile Computing, Networking and Communications (WiMob)*, pages 1–6, 2019.

- [13] H. Liu, H. Darabi, P. Banerjee, and J. Liu. Survey of wireless indoor positioning techniques and systems. *IEEE Transactions on Systems, Man, and Cybernetics, Part C (Applications and Reviews)*, 37(6):1067–1080, 2007.
- [14] S. Memon, M. M. Memon, F. K. Shaikh, and S. Laghari. Smart indoor positioning using ble technology. In *2017 4th IEEE International Conference on Engineering Technologies and Applied Sciences (ICETAS)*, pages 1–5, 2017.
- [15] C. S. Mouhammad, A. Allam, M. Abdel-Raouf, E. Shenouda, and M. Elsabrouty. Ble indoor localization based on improved rssi and trilateration. In *2019 7th International Japan-Africa Conference on Electronics, Communications, and Computations, (JAC-ECC)*, pages 17–21, 2019.
- [16] George Oguntala, Raed Abd-Alhameed, S. Jones, James Noras, Mohammad Patwary, and Jonathan Rodriguez. Indoor location identification technologies for real-time iot-based applications: An inclusive survey. *Computer Science Review*, 30:55–80, 11 2018.
- [17] Francisco Fernandes Pimenta. Indoor location based on aoa and bluetooth low energy. Master’s thesis, Faculty of Engineering, University of Porto, 7 2020.
- [18] Matthew Rhudy, Roger Salguero, and Keaton Holappa. A kalman filtering tutorial for undergraduate students. *International Journal of Computer Science & Engineering Survey*, 08:01–18, 02 2017.
- [19] M. E. Rida, F. Liu, Y. Jadi, A. A. A. Algawhari, and A. Askourih. Indoor location position based on bluetooth signal strength. In *2015 2nd International Conference on Information Science and Control Engineering*, pages 769–773, 2015.
- [20] M. Salimibeni, Z. Hajiakhondi-Meybodi, P. Malekzadeh, M. Atashi, K. N. Plataniotis, and A. Mohammadi. Iot-td: Iot dataset for multiple model ble-based indoor localization/tracking. In *2020 28th European Signal Processing Conference (EUSIPCO)*, pages 1697–1701, 2021.
- [21] P. Spachos and K. N. Plataniotis. Ble beacons for indoor positioning at an interactive iot-based smart museum. *IEEE Systems Journal*, 14(3):3483–3493, 2020.
- [22] Zain Tariq, Dost Cheema, Muhammad Kamran, and Ijaz Naqvi. Non-gps positioning systems: A survey. *ACM Computing Surveys*, 50:1–34, 08 2017.
- [23] Johannes Traa. Least-squares intersection of lines. *UIUC*, 2013.
- [24] Greg Welch and Gary Bishop. An introduction to the kalman filter. *Proc. Siggraph Course*, 8, 01 2006.
- [25] F. Zafari, A. Gkelias, and K. K. Leung. A survey of indoor localization systems and technologies. *IEEE Communications Surveys Tutorials*, 21(3):2568–2599, 2019.